

## Durham Research Online

---

### Deposited in DRO:

22 October 2021

### Version of attached file:

Draft Version

### Peer-review status of attached file:

Peer-reviewed

### Citation for published item:

Talling, Peter and Baker, Meg and Pope, Ed and Cula, Costa and Cartigny, Matthieu and Faria, Rui and Clare, Michael and Simmons, Steve and Silva Jacinto, Ricardo and Heijnen, Maarten and Hage, Sophie and Heerema, Catharina and Ruffell, Sean and McGee, Claire and Hasenhündl, Martin and Apprioual, Ronan and Gaillot, Arnaud and Wallace, Dec and Griffiths, Allan and Tshimanga, Raphael and Bola, Gode and Trigg, Mark and Robertson, Rick and Urlaub, Morelia and Parsons, Dan and Nambala, Laldemira and Nunny, Robert (2021) 'Novel sensor array helps to understand submarine cable faults off West Africa.', Working Paper. UNSPECIFIED.

### Further information on publisher's website:

<https://doi.org/10.31223/X5W328>

### Publisher's copyright statement:

### Additional information:

White paper prepared for International Cable Protection Committee

---

### Use policy

The full-text may be used and/or reproduced, and given to third parties in any format or medium, without prior permission or charge, for personal research or study, educational, or not-for-profit purposes provided that:

- a full bibliographic reference is made to the original source
- a [link](#) is made to the metadata record in DRO
- the full-text is not changed in any way

The full-text must not be sold in any format or medium without the formal permission of the copyright holders.

Please consult the [full DRO policy](#) for further details.

## Cover Page

*This paper has not been formally peer-reviewed and may be submitted for publication in a peer-reviewed journal in the near future. Subsequent versions of this manuscript may vary in content and length. If published, the final version will be included with a link on the peer-reviewed publication doi page.*

### Novel sensor array helps to understand submarine cable faults off West Africa

White Paper report by: Peter J. Talling<sup>1\*</sup> (Peter.J.Talling@durham.ac.uk), Megan L. Baker<sup>1</sup> (megan.l.baker@durham.ac.uk), Ed L. Pope<sup>1</sup> (ed.pope@durham.ac.uk), Matthieu J. B. Cartigny<sup>1</sup> (matthieu.j.cartigny@durham.ac.uk), Costa A. Cula<sup>2</sup> (costa.cula@angolacables.co.ao), Rui Faria<sup>2</sup> (rui.faria@angolacables.co.ao), Michael A. Clare<sup>3</sup> (michael.clare@noc.ac.uk), Steve M. Simmons<sup>4</sup> (S.Simmons@hull.ac.uk), Ricardo Silva Jacinto<sup>5</sup> (ricardo.silva.jacinto@ifremer.fr), Maarten S. Heijnen<sup>6</sup> (maarten.heijnen@noc.ac.uk), Sophie Hage<sup>5,7</sup> (sophie.hage1@ucalgary.ca), Catharina J. Heerema<sup>1</sup> (heerema.kate@gmail.com), Sean Ruffell<sup>1</sup> (sean.ruffell@durham.ac.uk), Claire McGee<sup>8</sup> (c.a.mcgee2@newcastle.ac.uk), Martin Hasenhündl<sup>9</sup> (martin.hasenhuendl@tuwien.ac.at), Ronan Apprioual<sup>5</sup> (Ronan.Apprioual@ifremer.fr), Anthony Ferrant<sup>5</sup> (anthony.ferrant@ifremer.fr), Arnaud Gaillot<sup>5</sup> (arnaud.gaillot@ifremer.fr), Dec Wallace<sup>10</sup> (dec.wallace@bt.com), Allan Griffiths<sup>11</sup> (allan.griffiths@vodafone.com), Raphael Tshimanga<sup>12</sup> (raphtm@yahoo.fr), Gode Bola<sup>12</sup> (gode.bola@gmail.com), Mark A. Trigg<sup>13</sup> (M.Trigg@leeds.ac.uk), Rick Robertson<sup>2</sup> (Rick@atmosphere.co.za), Morelia Urlaub<sup>14</sup> (murlaub@geomar.de), Dan R. Parsons<sup>4</sup> (D.Parsons@hull.ac.uk), Ducerolde Carlos Nunes Neto<sup>15</sup> (nunesneto@yahoo.com), Tresor Illola Jorge<sup>16</sup> (ilolajorge88@gmail.com), Laldemira Nambala<sup>17</sup> (laldemira.nambala@mtti.gov.ao), Robert Nunny<sup>18</sup> (robnunny@hotmail.com), Christine Peirce<sup>1</sup> (christine.peirce@durham.ac.uk), Richard Burnett (richard.burnett@newcastle.ac.uk)<sup>19</sup>, Jeffrey Neasham<sup>19</sup> (jeff.neasham@newcastle.ac.uk), and Nick G. Wright<sup>19</sup> (Nick.Wright@newcastle.ac.uk)

<sup>1</sup>Departments of Geography and Earth Science, Durham University, South Road, Durham, DH1 3LE, UK

<sup>2</sup>Angola Cables SA, Cellwave Building 2nd Floor Via AL5, Zona XR6B, Talatona - Luanda, Angola

<sup>3</sup>National Oceanography Centre Southampton, SO14 3ZH, UK & ICPC Marine Environmental Advisor

<sup>4</sup>Energy and Environment Institute, University of Hull, HU6 7RX, UK

<sup>5</sup>Marine Geosciences Unit, IFREMER Centre de Brest, Plouzané, France

<sup>6</sup>School of Ocean and Earth Sciences, University of Southampton, Southampton, SO14 3ZH, UK

<sup>7</sup>Department of Geosciences, University of Calgary, Calgary, Alberta T2N 1N4, Canada

<sup>8</sup>School of Civil Engineering and Geosciences, Newcastle University, Newcastle upon Tyne, UK

<sup>9</sup>Institute of Hydraulic Engineering and Water Resources Management, TU Wien, 1040 Vienna, Austria

<sup>10</sup>Subsea Centre of Excellence Technology, BT, UK

<sup>11</sup>O&M Submarine Engineering, Vodafone Group, Leeds, UK

<sup>12</sup>CRREBaC (Congo Basin Water Resources Research Center), University of Kinshasa, DR Congo

<sup>13</sup>School of Civil Engineering, University of Leeds, Leeds, LS3 9JT, UK

<sup>14</sup>GEOMAR Helmholtz Centre for Ocean Research, Wischhofstraße 1-3, 24148 Kiel, Germany

<sup>15</sup>Faculty of Sciences of the Agostinho Neto University, Av. 4 de Fevereiro 71, Luanda, Angola

<sup>16</sup>National Institute of Biodiversity and Conservation Areas (INBAC), Ministry of the Environment, Angola

<sup>17</sup>Angolan Ministry of Telecommunications and Information Technologies, Luanda, Angola

<sup>18</sup>Ambios, 1 Hexton Road, Glastonbury, Somerset, BA6 8HL, UK.

<sup>19</sup>School of Engineering, Newcastle University, Newcastle upon Tyne, NE1 7RU, UK.

\* Corresponding author's email: Peter.J.Talling@durham.ac.uk

# Novel sensor array helps to understand submarine cable faults off West Africa

White Paper report by: Peter J. Talling<sup>1\*</sup>, Megan L. Baker<sup>1</sup>, Ed L. Pope<sup>1</sup>, Matthieu J. B. Cartigny<sup>1</sup>, Costa A. Cula<sup>2</sup>, Rui Faria<sup>2</sup>, Michael A. Clare<sup>3</sup>, Steve M. Simmons<sup>4</sup>, Ricardo Silva Jacinto<sup>5</sup>, Maarten S. Heijnen<sup>6</sup>, Sophie Hage<sup>5,7</sup>, Catharina J. Heerema<sup>1</sup>, Sean Ruffell<sup>1</sup>, Claire McGee<sup>8</sup>, Martin Hasenhündl<sup>9</sup>, Ronan Apprioual<sup>5</sup>, Anthony Ferrant<sup>5</sup>, Arnaud Gaillot<sup>5</sup>, Dec Wallance<sup>10</sup>, Allan Griffiths<sup>11</sup>, Raphael Tshimanga<sup>12</sup>, Gode Bola<sup>12</sup>, Mark A. Trigg<sup>13</sup>, Rick Robertson<sup>2</sup>, Morelia Urlaub<sup>14</sup>, Dan R. Parsons<sup>4</sup>, Ducerolde Carlos Nunes Neto<sup>15</sup>, Tresor Illola Jorge<sup>16</sup>, Laldemira Nambala<sup>17</sup>, Robert Nunny<sup>18</sup>, Christine Peirce<sup>1</sup>, Richard Burnett<sup>19</sup>, Jeffrey Neasham<sup>19</sup>, and Nick G. Wright<sup>19</sup>

<sup>1</sup>Departments of Geography and Earth Science, Durham University, South Road, Durham, DH1 3LE, UK

<sup>2</sup>Angola Cables SA, Cellwave Building 2nd Floor Via AL5, Zona XR6B, Talatona - Luanda, Angola

<sup>3</sup>National Oceanography Centre Southampton, SO14 3ZH, UK & ICPC Marine Environmental Advisor

<sup>4</sup>Energy and Environment Institute, University of Hull, HU6 7RX, UK

<sup>5</sup>Marine Geosciences Unit, IFREMER Centre de Brest, Plouzané, France

<sup>6</sup>School of Ocean and Earth Sciences, University of Southampton, Southampton, SO14 3ZH, UK

<sup>7</sup>Department of Geosciences, University of Calgary, Calgary, Alberta T2N 1N4, Canada

<sup>8</sup>School of Civil Engineering and Geosciences, Newcastle University, Newcastle upon Tyne, UK

<sup>9</sup>Institute of Hydraulic Engineering and Water Resources Management, TU Wien, 1040 Vienna, Austria

<sup>10</sup>Subsea Centre of Excellence Technology, BT, UK

<sup>11</sup>O&M Submarine Engineering, Vodafone Group, Leeds, UK

<sup>12</sup>CRREBaC (Congo Basin Water Resources Research Center), University of Kinshasa, DR Congo;

<sup>13</sup>School of Civil Engineering, University of Leeds, Leeds, LS3 9JT, UK

<sup>14</sup>GEOMAR Helmholtz Centre for Ocean Research, Wischhofstraße 1-3, 24148 Kiel, Germany

<sup>15</sup>Faculty of Sciences of the Agostinho Neto University, Av. 4 de Fevereiro 71, Luanda, Angola

<sup>16</sup>National Institute of Biodiversity and Conservation Areas (INBAC), Ministry of the Environment, Angola

<sup>17</sup>Angolan Ministry of Telecommunications and Information Technologies, Luanda, Angola

<sup>18</sup>Ambios, 1 Hexton Road, Glastonbury, Somerset, BA6 8HL, UK.

<sup>19</sup>School of Engineering, Newcastle University, Newcastle upon Tyne, NE1 7RU, UK.

\* Corresponding author's email: Peter.J.Talling@durham.ac.uk

## Abstract

Seabed telecommunication cables can be damaged or broken by powerful seafloor flows of sediment (called turbidity currents), which may run out for hundreds of kilometres into the deep ocean. These flows have the potential to affect multiple cables near-simultaneously over very large areas, so it is more challenging to reroute traffic or repair the cables. However, cable-breaking turbidity currents that run out into the deep ocean were poorly understood, and thus hard to predict, as there were no detailed measurements from these flows in action. Here we present the first detailed measurements from such cable-breaking flows, using moored-sensors along the Congo Submarine Canyon offshore West Africa. These turbidity currents include the furthest travelled sediment flow (of any type) yet measured in action on Earth. The SAT-3 (South Atlantic 3) and WACs (West Africa Cable System) cables were broken on 14-16<sup>th</sup> January 2020 by a turbidity current that accelerated from 5 to 8 m/s, as it travelled for > 1,130 km from river estuary to deep-sea, although a branch of the WACs cable located closer to shore survived. The SAT-3 cable was broken again on 9<sup>th</sup> March 2020 due to a second turbidity current, this time slowing data transfer during regional coronavirus (COVID-2019) lockdown. These cables had not experienced faults due to natural causes in the previous 19 years. The two cable-breaking flows are associated with a major flood along the Congo River, which produced the

highest discharge (72,000m<sup>3</sup>) recorded at Kinshasa since the early 1960s, and this flood peak reached the river mouth on ~30<sup>th</sup> December 2019. However, the cable-breaking turbidity currents occurred 2-10 weeks after the flood peak and coincided with unusually large spring tides. Thus, the large cable-breaking flows in 2020 are caused by a combination of a major river flood and tides; and this can provide a basis for predicting the likelihood of future cable-breaking flows. Older (1883-1937) cable breaks in the Congo Submarine Canyon occurred in temporal clusters, sometimes after one or more years of high river discharge. Increased hazards to cables may therefore persist for several years after one or more river floods, which cumulatively prime the river mouth for cable-breaking flows. The 14-16<sup>th</sup> January 2020 flow accelerated from 5 to 8 m/s with distance, such that the closest cable to shore did not break, whilst two cables further from shore were broken. The largest turbidity currents may increase in power with distance from shore, and are more likely to overspill from their channel in distal sites. Thus, for the largest and most infrequent turbidity currents, locations further from shore can face lower-frequency but higher-magnitude hazards, which may need to be factored into cable route planning. Observations off Taiwan in 2006-2015, and the 2020 events in the Congo Submarine Canyon, show that although multiple cables were broken by fast (> 5 m/s) turbidity currents, some intervening cables survived. This indicates that local factors can determine whether a cable breaks or not. Repeat seabed surveys of the canyon-channel floor show that erosion during turbidity currents is patchy and concentrated around steeper areas (knickpoints) in the canyon profile, which may explain why only some cables break. If possible, cables should be routed away from knickpoints, also avoiding locations just up-canyon from knickpoints, as knickpoints move up-slope. This study provides key new insights into long runout cable-breaking turbidity currents, and the hazards they pose to seafloor telecommunication cables.

## **1. Introduction**

Seafloor fibre-optic telecommunication cable networks carry over 99% of global data traffic between continents, which includes the internet, financial trading, cloud data storage and voicemail, thereby underpinning the global economy and our day-to-day lives<sup>1</sup>. These cables can be damaged or broken by powerful seafloor flows of sediment, called turbidity currents, which runout on occasions for hundreds or thousands of kilometres into the deep-sea<sup>2</sup>. Turbidity currents carve some of the deepest canyons and longest channels on Earth, and form its largest sediment accumulations<sup>2,3</sup>. These flows are mixtures of sand and mud with seawater, which are denser than the surrounding ocean water, and thus flow along the seabed - sometimes at very high speeds<sup>2,4</sup>. For example, in 1929, a turbidity current travelling at up to 19 m/s broke all telegraph cables crossing the North Atlantic, and travelled for > 800km along the seabed offshore Newfoundland, Canada<sup>5,6</sup>. More recently, turbidity currents caused repeated cable breaks within the Gaoping Canyon offshore Taiwan in 2009-15. These flows had speeds of up to 20 m/s, and sustained speeds of 5 to 8 m/s for over 300 km<sup>1,7,8</sup>. Cable breaks due to the 2009 Gaoping Canyon event alone took 11 vessels to repair, causing data traffic to slow for 49 days<sup>1</sup>. This highlights that although most cable breaks occur due to vessel anchors or other activities in shallow water, turbidity currents can break numerous cables over very large areas, which take longer to repair, making it more challenging to reroute data traffic along alternative cable routes. Note that in this contribution we use *cable break* as a generic term to describe damage caused by external forces, as in Carter et al. (2014)<sup>1</sup>. Such damage may not necessarily lead to a complete break of the cable, and may just cause a loss in connection across the cable.

Despite their importance for offshore geohazards, or indeed global sediment and organic carbon transfer, there are remarkably few direct measurements of turbidity currents in action, so these sediment flows are poorly understood, and thus hard to predict<sup>3,9</sup>. Turbidity currents have been monitored in detail at fewer than 10 sites worldwide, and these flows were all in relative shallow (< 2 km) waters and ran out for less than ~50 km<sup>2, 9-14</sup>. However, there have previously been no detailed measurements from the most powerful and longest runout turbidity currents, which break cables and reach the deep ocean. The only measurements

from such long runout and powerful events were indeed restricted to the timings of cable breaks, and thus frontal transit speeds<sup>2,5</sup>.

This contribution presents the first detailed monitoring of powerful submarine turbidity currents that break seafloor telecommunication cables. These turbidity currents ran out for over 1,150 km into the deep-sea, making them the longest sediment flows (of any type) yet monitored in action on our planet. These unique field measurements come from the Congo Submarine Canyon and Channel located offshore West Africa, which extends from the mouth of the Congo River to water depths in excess of 4,750m (Fig. 1). Field data include detailed measurements of turbidity currents that broke the WACS (West Africa Cable System) and SAT-3 (South Atlantic 3) cables on January 14-16<sup>th</sup> 2020, and then broke the SAT-3 cable again on March 9<sup>th</sup> 2020 (Fig. 1). These cable breaks caused data transfer to slow significantly across large parts of Western and Southern Africa. Given the remote location and deep water of the Congo Canyon faults, it can take up to 15-20 days for a cable repair to be completed as the vessel needs to be mobilised, transit to the fault location and complete the deep water repair. For example, it took 20 days to repair the WACS cable after the 16<sup>th</sup> January break, by 6<sup>th</sup> February 2020. Angola Cables quickly rerouted WACS data traffic via a redundant link on SACS (South Atlantic Cable System) to mitigate disruption. In the case of the March 2020 event, the cable-break reduced internet speeds during coronavirus related lockdown across large parts of Western and Southern Africa, when data transfer was especially critical.

### *1.1 Aims*

Here we analyse the first detailed measurements from cable-breaking turbidity currents in action, which occurred in the Congo Submarine Canyon and Channel offshore West Africa (Fig. 1). Our overall purpose is to understand the implications of these measurements for assessing and mitigating the hazards to seabed telecommunication cables. This includes insights into how turbidity currents are triggered at river mouths, and hence their likely future frequency, including the impacts of climate change. An interesting observation is that one branch of the WACS cable survived both 2020 turbidity current events, despite being impacted by flows with frontal speeds of ~5 m/s. We thus also seek to understand why some cables are broken, whilst other cables remain unbroken.

## **2. Background**

The Congo Submarine Canyon extends from the estuary of the Congo River (Fig. 1), and it is one of the few submarine canyons worldwide where the canyon-head connects directly to a major river mouth (the Congo Estuary). Indeed, the head of the canyon lies about 30 km inside the estuary, where surveys indicate an abrupt increase in water depths from ~20 m to over 160 m<sup>15,16</sup>. This sinuous underwater canyon is incised deeply into the continental shelf and slope, before emerging from the base of the continental slope at ~3200 m water depth (Fig. 1a,b)<sup>17-19</sup>. The canyon then continues as a sinuous submarine channel that eventually terminates at a water depth of ~4,800 m (Fig. 1c), some 1,200 km from the river mouth (as measured along the canyon-channel's sinuous course). The term 'submarine canyon' is used here to denote a deeply eroded feature, with 'upper canyon' referring to the stretch in shallower water (< 2170 m), located closer to the coast (Fig. 1b). In contrast, 'submarine channels' are less-deeply incised, so that larger flows can overspill to deposit sediment on adjacent upraised banks called levees<sup>17,18</sup>. Submarine channels may be prone to channel switching (avulsions), as occurs in terrestrial rivers<sup>20,21</sup>. The area immediately beyond the channel mouth is termed the 'lobe', where flows expand and deposit substantial volumes of sediment<sup>22</sup>. The overall character of the Congo Submarine Canyon-Channel is well described by Babonneau et al. (2002, 2010), and other past work led by IFREMER<sup>19</sup>, which was based on the first complete mapping of such a large-scale submarine canyon-channel-lobe system. This work included mapping a complex sequence of >50 channel avulsions in

the last ~210,000 years<sup>20,21</sup>, as well as detailed analysis of sediment budgets and organic carbon burial rates within the lobe, which result in unique deep-sea ecosystems<sup>22-24</sup>.

### *2.1. Previous seabed cable routes and faults*

Early telegraphic communications cables (1883 to 1937) that crossed the Congo Submarine Canyon followed three routes across the upper canyon, at water depths of less than 2 km (Fig. 2a,b)<sup>15</sup>. Faults on these early cable routes were frequent, and they occurred most commonly during months in which the Congo River discharge was high (Fig. 2c)<sup>15</sup>. Early cable breaks also tended to occur in temporal clusters, sometimes after one or more years of high river discharge (Fig. 2b,d).

More recently, the SAT-3 (2001-onwards) and then WACS fiber-optic telecommunication cables (2012-onwards) were routed across the canyon, in more offshore locations (Fig. 1). The SAT-3 cable crosses at a water depth of ~3570 m, whilst the WACS cable has two branches, crossing the canyon at ~ 2,100 m and ~4,100m depth (Fig. 1a,b). SAT-3 and WACS cables had not previously been damaged by natural causes since a fault on SAT-3 on 9<sup>th</sup> October 2002 (01.23 UTC). This lack of cable-breaks in the preceding ~18 years suggests that the long runout turbidity currents that broke these cables in January and March 2020 were unusually powerful, as discussed more fully in later sections.

Plans are currently underway for further cable routes to West Africa, such as the Equiano cable to be routed to the north of the Congo Submarine Canyon-Channel, and the proposed 2Africa cable that will connect the entire African continent. A further (ACE - Africa Coast to Europe) cable had also been laid across the deep-water part of the Congo submarine channel. The ACE cable was also broken in early 2020, presumably by the January 2020 turbidity current. However, the ACE cable was not yet operational in January 2020, so that the exact timing of this cable break is unknown. Information outlined here may help in the design and planning of future cable routes.

### *2.2. Previous (pre-2019) turbidity current monitoring in Congo Submarine Canyon*

The Congo Canyon was one of the first sites where turbidity currents were monitored in action. Initial work by IFREMER involved propeller-based current meters attached to moorings, which recorded average flow speeds over an hour at a single height above the seabed<sup>11,25</sup>. This pioneering work showed that long runout (> ~400 km) flows occurred in March 2001 and January 2004. The March 2001 turbidity current badly damaged the mooring, which was recovered from the ocean surface, with its current meter recording hourly average internal flow speeds of 1.2 m/s. The January 2004 flow had a front speed of 3.5 m/s as it transited between moorings located at water depths of 3420 to 4070 m. The front of this flow then decelerated to 0.7 m/s between moorings at 4070 to 4790 m water depth (Fig. 6), and it failed to break the SAT-3 cable located at 3570 m.

Further pioneering turbidity current monitoring in the Congo Canyon was carried out in the upper Congo Canyon in 2009-10 and 2013<sup>13,26-28</sup>. These studies used moorings located at water depths of ~1850 m that contained downward-looking Acoustic Doppler Current Profilers (ADCPs) which were located 60 to 220 m above the canyon floor. ADCPs provide measurements of velocity and sediment concentration<sup>28</sup> in the water column. These moorings showed that turbidity currents were very common in the upper canyon, occurring 20 to 30 % of the time during deployments in 2009-10 and 2013 (Fig. 3). Individual turbidity currents had measured maximum velocities of 2.5 to 3 m/s, and could sustain internal velocities of ~1 m/s for 7-10 days (Fig. 3), making them far more prolonged than any previously measured turbidity currents<sup>13</sup>.

The turbidity currents in the Congo Canyon could be subdivided into short-lived (~30 min duration) frontal regions that were much faster moving, and thus ran away from, slower moving bodies and tails that often

lasted for several days (Fig. 3)<sup>13,28</sup>. The faster frontal region probably also has much higher sediment concentrations than the dilute bodies and tails (Fig. 3b)<sup>28</sup>, and it is this fast and dense frontal region that poses the greatest hazard to cables.

However, it was not known how far these upper-canyon turbidity currents in 2010-2013 ran out<sup>13,26-28</sup>, and they were not associated with any breaks on deeper-water cables routes. It thus appears that smaller scale (albeit still quite powerful) turbidity currents are very common in the upper Congo Canyon; however, much more powerful and longer turbidity currents that damage or sever cables (as in January and March 2020) are much more infrequent.

### **3. Methods**

This contribution is the first report on measurements made in 2019-20, which were part of a joint UK-Angola-French-German project. This project involved the UK Universities of Durham, Hull, Newcastle, Southampton and Leeds, UK National Oceanography Centre, IFREMER (Institut Français de Recherche pour l'Exploitation de la MER) in France and GEOMAR Helmholtz Centre for Ocean Research based in Germany; and was co-led by Angola Cables. This project deployed an array of 10 oceanographic moorings from September 2019 to January 2020 along the Congo Canyon and Channel (Figs. 1 & 4). Each mooring contained one or two ADCPs, together with CTD (conductivity, temperature and depth) sensors that measured water temperature and salinity (Fig. 4). Each mooring had a 1,000 kg (in air) anchor, linked to a buoyant float via chain and wire (Fig. 4). These ADCPs were located 44 to 250 m above the seabed, and measured velocity profiles to the seabed every 9 to 45 seconds. Sediment traps were located on four moorings, at 22 to 40 m above seabed. The mooring array is summarised in Figure 4.

Seven moorings were located on the floor of the upper Congo Canyon at water depths of 1,575 to 2,200 m (Fig. 1b), and four moorings were deployed in the distal submarine channel at water depths of 4,030 to 4,730m (Fig. 1c). The original plan was to recover the moorings by triggering twin acoustic releases (Fig. 4). However, two moorings surfaced after their anchor-wire was broken by a turbidity current on 10<sup>th</sup> October 2019, one further mooring surfaced after a flow on 27<sup>th</sup> December 2019, whilst the remaining seven moorings all surfaced during the powerful (cable-breaking) turbidity current on 14-16<sup>th</sup> January 2020 (Fig. 5). Recovering the moorings that were drifting on the sea-surface was extremely challenging. We are very grateful for assistance in mooring recovery by vessels including the RV Thevenin, Thor Frigg, Maria Francisca, and Helena; as well as a range of colleagues including those at Vodafone, Orange, BT, and others, as is set out fully in Appendix 1.

Finally, time-lapse surveys of seabed morphology were completed in both 2019 and 2020 using an EM122 swath multibeam system. These surveys covered the floor of the upper canyon and the distal submarine channel (Fig. 1). IFREMER have previously collected bathymetric surveys across the entire submarine-canyon-channel-lobe system in 1998-2000<sup>17-19</sup>. These time-lapse surveys document seabed change<sup>29</sup>, and some initial results are presented herein.

#### **3.1. Identifying turbidity current events and frontal (transit) speeds**

Turbidity currents were identified within ADCP data via an abrupt increase in near-seabed velocities. This method gave the precise time at which turbidity currents reached each mooring, up until the powerful 14-16<sup>th</sup> January 2020 turbidity current, which caused the final seven moorings to surface (Fig. 5). Not all moorings were present in the canyon-channel for the entire period up until 14-16<sup>th</sup> January 2020, as three moorings had previously surfaced on 10<sup>th</sup> October or 27<sup>th</sup> December 2019 (Fig. 5). Flow arrival times at moorings were combined with times of faults on the SAT-3 and WACs cables, and distances measured along the axis of the canyon-channel, to derive flow front (transit) speeds between various moorings and cables (Fig. 6).

### *3.2. Congo River discharge and tidal cycles*

The timing of turbidity currents was compared to fluctuations in water discharge from the Congo River at the Kinshasa gauging station, located ~ 400 km from the river mouth, as measured by the Regie des Voies Fluviales (RVF) at Kinshasa, Democratic Republic of Congo. River discharge data included a major flood that peaked on 27<sup>th</sup> December 2019 (Fig. 7a,b). Daily tidal data were obtained for Santo Antonio do Zaire near the port of Soyo, at the Congo River mouth<sup>30</sup> ( Fig. 7c).

## **4. Results: Observations in 2019-2020**

### *4.1. Cable-breaking turbidity current on 14-16<sup>th</sup> January 2020*

On 14-16<sup>th</sup> January 2020, a turbidity current travelled along the Congo Submarine Canyon, broke the SAT-3 and WACS telecommunications cables, and caused the remaining seven ADCP-moorings to surface (Figs. 5 & 6). However, the shallower-water branch of the WACS cable did not display any break (Fig. 5). Arrival of this turbidity current was recorded by the ADCPs on seven moorings, although the mooring wires then broke, such that moorings rose to the ocean surface. Timings of cable breaks and flow arrival times measured by the ADCPs allow the transit (flow front) speed between these various cable and mooring sites to be calculated, using the distance measured along the sinuous canyon or channel axis (Fig. 6) This method assumes that the cables were broken on flow arrival, as was the case for the ADCP-mooring's anchor-cables. This analysis shows a turbidity current reached the shallowest water ADCP-mooring at 22:31 UTC on 14<sup>th</sup> January 2020, and arrived at the final deep-water ADCP-mooring at 21.01 UTC on 16<sup>th</sup> January. The flow front initially travelled at 5.2 m/s in the upper canyon, but then continuously accelerated to a speed of 8 m/s by the end of the channel at water depths of 4,500 to 4,730 m (Fig. 6). This turbidity current ran out for over 1,130 km from the river mouth, as measured along the sinuous canyon-channel course.

### *4.2. Cable-breaking turbidity current on 9<sup>th</sup> March 2020*

The SAT-3 cable broke again on 9<sup>th</sup> March 2020, at the same canyon-floor location as the break in January 2020, although the two branches of the WACS cable continued to function. The coincident location of the SAT-3 break, where it crosses the floor of the canyon, suggests that the 9<sup>th</sup> March break was due to a second powerful and long runout turbidity current.

During the Jan 2020 repair of the SAT-3 cable, 3.8 km cable was abandoned on the seabed due to high tensions during recovery. This suggests that the some of the cable was trapped and buried by sediment deposited by the January turbidity current. During the March 2020 repair, all of the SAT-3 cable was recovered. However, tensions during cable recovery suggested that the cable was buried, and then unburied by the vessel during recovery. A 700m section of cable suffered abrasive gouge-mark damage.

### *4.3. Slower and shorter runout turbidity currents that failed to damage cables*

The ADCP-moorings recorded 12 additional turbidity currents that had slower transit speeds than the 14-16<sup>th</sup> January event (Fig. 5, 6). Only one of these flows (8<sup>th</sup> January) appears to have runout for more than 900 km, to reach the array of four moorings along the distal channel (Fig. 6). This flow travelled at 4.4 m/s initially, before slowing markedly to speeds of <0.5 m/s. The remaining flows were only recorded by ADCP-moorings in the upper canyon, at water depths shallower than 2,172 m (Fig. 5, 6). However, it is possible that these events ran out past the WACS and SAT-3 cable crossings without damaging the cables, but they did not reach the ADCP-mooring at 4,036 m water depth (Fig. 5). These smaller flows had speeds of < 3.8 m/s, and their transit speeds decelerated along their pathway (Fig. 6).

### *4.4. Patterns of seabed erosion from time-lapse surveys*



Surveys of the channel-canyon floor show a series of knickpoints (local steepening of the long profile of the canyon-channel)<sup>17,18</sup>. Comparison between the 1998-2000 and 2019 surveys also show that a major (0.1 km<sup>3</sup>) landslide had blocked the upper canyon at some time between 2000 and 2019, which dammed a further 0.5 km<sup>3</sup> of sediment (Fig. 8)<sup>29</sup>. This dammed sediment forms a wedge that is up to 150 m thick, and extends for over 26 km up-canyon<sup>29</sup>. Since 2019, erosion has started to cut a narrower channel through this landslide dam and sediment wedge (Fig. 8).

Analysis of changes in seabed elevation between 2019 and 2020 are still underway, but initial work suggests there was substantial erosion by the turbidity current events, with over 1 km<sup>3</sup> of sediment eroded along the surveyed canyon-channel reaches. For comparison, the annual global sediment supply from rivers to the ocean is about 7 km<sup>3</sup><sup>31</sup>. This erosion is mainly focussed on the canyon-channel floor, but it is not evenly distributed. Relatively deep (up to 30 m) stretches of erosion occurred around knickpoints.

## **5. Discussion and wider implications for hazards to cables**

### **5.1. Recent cable-breaking turbidity currents: preconditioned by major floods and triggered at spring tides**

The two powerful turbidity currents in January and March 2020 are associated with an exceptional flood along the Congo River, which had a peak discharge of ~72,000 m<sup>3</sup> at Kinshasa on 27<sup>th</sup> December 2019 (Fig. 7b). It is likely that the flood peak occurred by 30<sup>th</sup> December at the river mouth, an estimated delay of around 2-3 days from the gauge station in Kinshasa (M. Trigg, pers comm., 2019). This is the largest flood along the Congo River since the early 1960's (Fig. 7a), and this suggests that the cable-breaking flows in 2020 are associated with this 1 in 50 year flood<sup>32</sup>, especially as neither the SAT-3 or WACS cables had been broken in the preceding 19 years (since 2001).

However, the cable-breaking turbidity currents in 2020 did not coincide with peak flood discharge at the river mouth around 30<sup>th</sup> December, but instead occurred ~2 weeks (14-16<sup>th</sup> January event) and ~10 weeks (9<sup>th</sup> March event) after the flood peak. There was thus a significant delay between the river flood peak and these turbidity currents (Fig. 7a). Initiation of the two cable-breaking turbidity currents also coincides with the timing of unusually large spring tides (Fig. 7c). We therefore propose that a river flood with an annual exceedance probability of ~2% ('1 in 50 year') rapidly deposited a large amount of sediment in the estuary. This sediment was then released during large spring tides that occurred 2 and 10 weeks later (Fig. 7c,d), such that major cable-breaking turbidity currents are preconditioned by sediment supply from major river floods, and then finally triggered at spring tides.

### **5.2. Recent smaller-scale turbidity currents in the upper Congo Canyon**

The timing of the smaller turbidity currents in the upper canyon can also be compared to tidal cycles and river discharge (Fig. 7). However, this analysis is complicated by potentially significant time delays between when turbidity currents initiate at the estuary, and when they arrive at the first moorings located 102 km from the canyon-head in the estuary (Fig. 1). This time delay depends on the flow's speed, and it is only a few hours for fast moving (~5 m/s) turbidity currents, as was probably the case for major cable-breaking flows in 2020. Thus, faster flows are compared with confidence to spring-neap tides occurring every two weeks, if not individual low or high tide times. However, for a slower flow travelling at 0.5 m/s, it would take ~2.3 days to travel 100 km from the estuary to the first mooring. This means that comparisons between the timing of smaller flows and spring-neap tidal cycles are less confident than for faster cable breaking flows (Fig. 7).

If the first available transit speed is used to estimate the time at which flows were triggered in the estuary, with the uncertainties noted above, then smaller flows in 2019-2020 are more likely to be triggered on days

with larger tidal ranges (Fig. 7d), although there are notable exceptions (e.g. on 10<sup>th</sup> October 2019). The ADCP-moorings were only present in the canyon from September-October 2019 to 14<sup>th</sup> January 2020, during months with elevated river discharge. However, some smaller flows (e.g. 10<sup>th</sup> October 2019) occurred during periods with relatively low river discharge (Fig. 7a,e), such that the relationship between triggering of smaller flows and tides appears weaker than that for the two major cable-breaking flows (Fig. 7c). Non-cable breaking turbidity currents monitored in 2019-2020 (Fig 7b), and flows previous monitored in the upper canyon in 2010-13<sup>13,26,27</sup> and deep-water<sup>11,25</sup> also occurred at a rather wide range of river discharges (Fig. 7e).

### 5.3. Earthquakes

Earthquakes are infrequent along this passive margin. Only two significant (> Mw ~2.5) earthquakes were noted during the 2019-2020 sensor deployment, on 19<sup>th</sup> December 2019 in the Gulf of Guinea, and on 21<sup>st</sup> November 2019 in Namibia<sup>33</sup>. These earthquakes do not coincide with either cable-breaking flows on 14-16<sup>th</sup> January 2020 and 9<sup>th</sup> March 2020, or with smaller turbidity currents.

### 5.4. Older (1883-1937) cable breaking turbidity currents in the upper Congo Canyon

Cable breaks from 1883-1937 likely record turbidity currents in the upper canyon (Fig 2). These older cable-breaks tended to occur more commonly in some months of the year, albeit with much scatter (Fig. 2c). Thus, there is a weak relationship between months with elevated river discharge and more frequent turbidity currents, which were powerful enough to break those older cables (Fig. 2)<sup>15</sup>. This again suggests that elevated sediment supply to the estuary plays a role in triggering turbidity currents, although some events occurred long after the flood peak in December. However, this is a broad relationship, and some turbidity currents occur during periods of relatively low river discharge, as again seen in 2019-2020 (Fig. 7c).

### 5.5. Physical processes that generate turbidity currents in the river-mouth estuary

Observations from the Congo Estuary, especially offshore from the port of Soyo, provide some constraints on how turbidity current triggering may be favoured by either river floods or spring tides. However, they also show there is a compelling need for further monitoring effort in the estuary to test competing models.

The head of the Congo Submarine Canyon lies around 35 km inland from the mouth of the estuary, where water-depths suddenly increase from ~20 to ~160 m (Fig. 9)<sup>34</sup>. Freshwater from the river forms a surface plume with lenticular cross-section. A strongly developed halocline (change in salinity) separates this fast-moving and seaward-flowing plume of near-fresh water, from underlying slow-flowing seawater. Little information is available on the landward extent of the saline intrusion at different times of the year, or through individual tidal cycles<sup>16</sup>. However, increased river discharge and ebb (falling) tides favour the transport of bedload over the submarine canyon-lip. The surface plume mixes with seawater, and carries finer sediment into the lower estuary, and into the open ocean<sup>34</sup>.

There are three distinct sources of sediment transfer into the head of Congo Canyon, each of which could trigger turbidity currents (Fig. 9). The river's bedload (primarily sand) is probably the principle source of sediment. For example, Peters et al. (1978) calculated an annual bedload flux of ~150 Mt/yr in the lower part of the Congo River, which compares to an estimated suspended load of ~43 Mt/yr<sup>34</sup>, although there are major uncertainties in both estimates. The rate at which bedload is transported over the submarine canyon's lip is strongly dependent on both river discharge and tidal cycles. For example, based on field measurements near the canyon lip, Peters et al. (1978) estimated that a 10-fold increase in bedload discharge will occur if water discharge increased from 50,000 to 70,000 m<sup>3</sup>. Peters et al. (1978) also showed that much greater bedload discharge occurred towards the canyon lip during ebb tides, which is likely to be accentuated during the strongest spring tides. It is thus highly plausible that river floods and spring tides combine to produce

unusually rapid progradation of the submarine canyon's lip, thereby triggering turbidity currents via slope failure, as in other systems<sup>35,36</sup>.

The second source of muddier sediment comes via settling from the surface plume of freshwater originating from the Congo River. This surface river plume hugs the southern shore of the estuary at all times, under the influence of the Coriolis effect or other processes. This plume therefore tends to lie above an extensive (30 km<sup>3</sup>) shallow-water plateau located near to the port of Soyo (Fig. 9). Thus, the muddy suspended load from the river is separated effectively from the main submarine canyon-head, which receives the sandy bedload. During periods of the year with lower river discharge, the shallow-water plateau offshore from Soyo becomes a site of sustained mud deposition, appearing to accommodate about half of the river's suspended load (i.e. ~20M t yr<sup>-1</sup><sup>34</sup>). With the onset of higher Congo River discharges, the freshwater plume from the river then expands to touch-down onto the seabed across the plateau, which mobilises this mud-deposit. This process generates thin (~1 m) fluid-mud layers that move seawards (R. Nunny, pers. comm.). Such fluid-mud flows tend to occur at particularly low spring-tides, and when the river discharge is high (November to January), and they are best developed in December when fluid-mud flows can occur for over 10% of the time. Fluid-mud flows generated in this way then runout into a major tributary canyon (canyon 5; Fig. 9) to the main Congo Canyon. Active slumping also occurs in all these tributary canyons at depths of 20-50 m (R Nunny, pers comm). It is thus also highly plausible that increased river discharge and tides combines to trigger turbidity currents through the formation of these fluid mud layers.

A third source of sediment for the Congo Canyon is the littoral drift that travels northwards along the ocean coast, interacting with the Congo River outflow at the Ponta do Padrão (Fig 9). Although this littoral drift supplies 200,000 m<sup>3</sup> of medium sand each year, it is much less substantial than sediment supply from the river. Much of this littoral sand is again fed into tributary canyons (canyons 4 and 5 in Fig. 9) to the main Congo Canyon, mainly at times of large ocean swells, typically during July and August. It thus appears that this littoral sand supply plays a more minor role in triggering turbidity currents down the Congo Canyon, which are more frequent in other months, and tend to coincide with factors other than ocean swell heights.

#### *5.6. What controls turbidity current transit speeds, self-acceleration and runout distance?*

Hazards to offshore cables depend both on initial turbidity current triggering and how flows then behave, as this determines their speeds, impact forces on cables, and final runout distance. This unusual data set allows us to start testing models for how turbidity currents evolve with distance. It has been proposed that turbidity currents that erode the seabed, and pick up additional sediment, become denser and thus faster. Faster flows would then erode even more sediment, and become even faster. This positive feedback and self-acceleration has been termed 'ignition'<sup>37</sup>. Conversely, when turbidity currents deposit sediment, they become less dense and thus slower, leading to more sediment settling, and further deceleration. This feedback has been termed 'dissipation'. A final 'autosuspension' model is that turbidity currents reach a near-equilibrium state, where erosion and deposition are balanced, such that flows maintain a near-uniform velocity<sup>37</sup>.

Here we present the first confirmation that full-scale oceanic turbidity currents can indeed self-accelerate and ignite over exceptionally long (> 1,000 km) distances (Fig. 6). The self-acceleration by the 14-16<sup>th</sup> January turbidity current from 5 to 8 m/s was not due to changes in seabed gradient, which decreases with distance. It is also not due to narrowing of the channel, which has a relatively uniform width<sup>17</sup>. Indeed, the channel becomes shallower with distance, promoting overspill and deceleration not acceleration. This means that acceleration of the 14-16<sup>th</sup> January turbidity current was most likely due to erosion of the seabed, and this is also consistent with very large volumes (> 1 km<sup>3</sup>) of canyon-channel floor erosion observed between the 2019 and 2020 seafloor surveys.

We can also compare spatial patterns in flow speeds with those recently reported for turbidity currents in Monterey Canyon, offshore California, where turbidity current behaviour tends to bifurcate. Initially faster flows ( $> 5$  m/s) have near uniform speeds of 5-8 m/s for tens of kilometres, whilst turbidity currents that are initially only fractionally slower decelerate and dissipate<sup>38</sup>. Small changes in the initial flow speed are thus linked to profound changes in how these flows then behave<sup>38</sup>. A broadly similar trend occurs for these turbidity currents in the Congo Canyon, albeit over much longer (100 to  $>1,100$  km not  $< 50$  km) runout distances (Fig. 6). Flows that are initially faster than 5 m/s tend to self-accelerate and ignite, albeit gradually, and maintain their power for much longer distances. Turbidity currents that have initial front speeds of  $< 4$  m/s tend to decelerate, and die out within the upper canyon (Fig. 6). It is these initially faster, and then continuously igniting turbidity currents, which pose the greater natural hazard to submarine cables.

## **6. Wider implications for future hazards to submarine cables**

In general, seafloor cable routes are chosen to avoid submarine canyons where possible. However,  $\sim 2.8\%$  of the total (1.8 million km) length of subsea telecommunication cables still cross submarine canyons (M. Clare, pers. comm., 2021). It is therefore not always possible to avoid submarine canyon-channels, particularly where they are as spatially extensive as the Congo Canyon and Channel, so that this study provides valuable information for planning of routes that necessitate a canyon or channel crossing. We now outline the wider implications of this study for assessing and mitigating hazards to submarine cables, both along the Congo Submarine Canyon and more generally for other river-fed canyon settings.

### **6.1. Flow triggering by major river floods and spring tides**

Regardless of the exact mechanism for triggering turbidity currents at the river mouth, cable-breaking flows appear to be associated with exceptional floods along the Congo River, and then finally triggered by spring tides after a delay of 2-10 weeks from the flood peak (Fig. 7). The only cable-breaking turbidity currents since 2001 came soon after a flood discharge of  $>70,000$  m<sup>3</sup>/s (Fig. 7a). During this period, peak annual river discharges of 40-60,000 m<sup>3</sup>/s did not produce cable-breaking flows (Fig. 7a). The January and March 2020 events suggest that individual extreme floods may deposit sufficient sediment at the river-estuary to generate multiple cable breaking flows over the following months (Fig. 6). Thus, elevated risk from turbidity currents may persist for a significant period after the flood peak, and after an initial long runout cable-breaking turbidity current. It may therefore be prudent to include an assessment of the recent flood history along the Congo River<sup>32</sup> in order to evaluate fluctuating levels of risk to the offshore cable systems, and the global positioning of cable repair vessels. Future changes in water discharge and sediment supply along the Congo River due to climate or land-use change also need to be predicted, given these potentially strong links between major river floods and cable-breaking turbidity currents. There may also be similar links between river floods, tidal cycles and turbidity currents offshore from other river mouths, affecting hazards to submarine cables in these more widespread locations.

### **6.2. Temporal clustering of multiple cable-breaking flows**

Analysis of the older cable breaks, from 1883 to 1937, provide an even longer record to interrogate about how cable-breaking flows are linked to river discharge, although these cable routes are located closer to the coast than the WACS and SAT-3 cables (Fig. 2)<sup>15</sup>. This longer record suggests that clusters of multiple cable breaks can sometimes occur for several years after one or more years of elevated Congo River discharge, albeit to levels below that seen in the 2020 flood, such as from 1925-29 (Fig. 2d). However, these turbidity currents may not have reached deeper water cable routes. It should also be noted that other periods of frequent cable breaks (e.g. 1900-1903; Fig. 2) are not associated with elevated river discharge. Additionally, the design and resilience of these telegraphic cables differs from the more modern fibre-optic

telecommunications laid in the last 20 years<sup>39</sup>. The generation of cable-breaking turbidity currents could depend on the cumulative sediment supply rates across multiple years, not just one flood, and there are compelling reasons to monitor the Congo River mouth in more detail.

### *6.3. Turbidity current self-acceleration and changes in hazards to cables with distance from shore*

The overall frequency of turbidity currents decreases strongly with distance as initially slower events dissipate within the upper canyon (Figs. 5 & 6). For example, turbidity currents were active for up to 33% of the time at 2 km water depth in the upper canyon, over periods of a few months (Fig. 3)<sup>13,28</sup>. Only two turbidity currents were recorded in the distal deep-water channel from September 2019 to January 2020. It is possible that this part of the system may not have any turbidity currents in some years.

However, the January 2020 event also shows that infrequent and longer runout turbidity currents may self-accelerate with distance, such that their frontal speeds increase from 5 to 8 m/s (Fig. 6). Thus, at least for these larger and more infrequent type of event, there may be an increased hazard to cables located further from shore, as they will experience the fastest flow front speeds during such events. Indeed, for the January 2020 turbidity current, the shallower water branch of the WACS cable was undamaged, whilst the deeper-water branch broke (Figs. 1 & 6). Moreover, flows in these distal deeper water sites travel through a channel that is less deeply incised into the surrounding seafloor<sup>17,18</sup>, such that flows may be more likely to overspill from the channel, and bury or damage cables. Cables may need to be routed away from the deeper water submarine channel, if they are to avoid damage from infrequent but much more powerful and long runout turbidity currents linked to major river floods.

### *6.4. Turbidity current speeds that do (or do not) cause cable breaks*

This study suggests that turbidity currents with frontal (transit) speeds in excess of ~5.5-6 m/s are needed to break cables, whilst cables (e.g. upper branch of WACS) can sometimes survive frontal speeds of up to 5 m/s (Fig. 6). This is broadly consistent with information from cable breaks along the Gaoping Canyon offshore Taiwan in several events from 2006-10, where transit speeds in excess of 5.5 m/s broke cables<sup>1,7,8</sup>.

However, another notable feature of these powerful turbidity currents in Gaoping Canyon is that although numerous cables were broken, a significant number of intervening cables remained unbroken during the same turbidity current event, despite presumably experiencing similar flow speeds of > 5 m/s<sup>1,7,8</sup>. Thus, there are local conditions that sometimes prevent some cables from breaking, whilst neighbouring cables do break. This in turn suggests that there may be ways to route cables in more advantageous positions within submarine canyons to reduce cable breaks, and it is not a foregone conclusion that cables will break in a turbidity current with a frontal speed over ~5 m/s.

Time-lapse surveys of the Congo Canyon and Channel may provide an explanation for why local factors cause some cables to break, whilst other cables survive these fast-moving flows. These surveys show that seabed erosion during turbidity currents may be very patchy, over distances of just a few kilometres (Fig. 8). In particular, deep (20-40 m) erosion may be associated with knickpoints, defined as zones of locally steeper gradients along the canyon or channel floor. A broadly similar pattern of erosion has been observed in time-lapse surveys of other submarine channels, such as in Bute Inlet in Canada, where erosion was focussed around knickpoints<sup>40</sup>. Bute Inlet knickpoints migrate rapidly upslope (up to ~500 m/yr), and are caused by internal flow-seabed processes, rather than external processes such as faults or bedrock ridges. Conversely, deposition of sediment can occur upstream of landslide dams, and this thick sediment accumulation could bury and protect cables from abrasion (Fig. 8)<sup>29</sup>.

These localised patterns of erosion and deposition may explain why some submarine cables break, whilst neighbouring cables do not break, as along the Gaoping or Congo Canyons<sup>7</sup>. This model can also provide a basis for deciding which sites to avoid for cable routes across canyons. It may be good to avoid crossing routes on knickpoints, or immediately up-slope from the knickpoint - as it may migrate and incise deeply. Further time-lapse surveys of local erosion and deposition within canyons and channels may help to determine their controls, and help locate future cable routes in more favourable sites.

## **7. Conclusions**

Here we outline the most detailed measurements yet from turbidity currents that break submarine cables, in order to understand the hazards turbidity currents pose to seabed telecommunication cables, and how those hazards can best be mitigated in the future. Two cable breaking flows occurred in the Congo Submarine Canyon on 14-16<sup>th</sup> January and 9<sup>th</sup> March 2020, some 2-10 weeks after a 1 in 50-year (2% annual exceedance probability) flood along the Congo River, and coincident with unusually large spring tides. It thus appears that these cable-breaking flows were preconditioned by rapid deposition of flood sediment at the river mouth, and finally triggered by spring tides, although further monitoring of the river mouth is needed to determine the exact triggering mechanism. Older cable breaks (1883-1937) in the upper canyon also occurred in temporal clusters, sometimes after one or more years of elevated river discharge, albeit less extreme than in 2019-2020. River floods may thus potentially provide an early warning that hazards from turbidity currents to offshore cables are increased, and hazards to offshore cables will be affected by future climate change and resulting changes in river flood frequency or magnitude. The 14-16<sup>th</sup> January turbidity current's front progressively accelerated from 5 to 8 m/s, as it flowed ~1,100km into the deep ocean. It also tended to overspill from the deeper-water channel, which is less deeply incised into the seafloor. Turbidity currents are much more common closer to shore (at canyon floor water depths of < 2,200m), sometimes occurring for ~30% of the time in the upper canyon<sup>13</sup>, such that hazards are typically much greater for canyon-crossing cable routes located closer to shore. However, during the exceptionally large turbidity currents such as in January and March 2020, cable routes located further offshore may face an increased hazard from faster flow speeds and overspill. Turbidity currents with front speeds faster than ~5 m/s broke telecommunication cables in this study, and in previous events that broke cables offshore Taiwan in 2006-2015. However, these observations show that although some cables broke, some intervening cables failed to break, despite also being impacted by flows moving at > 5 m/s. Thus, local effects - other than flow speed, can determine whether a cable breaks. This study shows that sometimes deep (> 30 m) seafloor erosion by turbidity currents is patchy. Deep-erosion is often associated with areas of steeper floor (called knickpoints), which migrate up-slope due to turbidity currents. Localised erosion at knickpoints may potentially explain why only some cables break in faster flows. This hypothesis suggests that cable routes should be located away from knickpoints, or areas immediately upslope from knickpoints, where cables will have a greater chance of surviving powerful turbidity currents. Detailed (and ideally time-lapse) bathymetric surveys may thus be used to identify the positions of active knickpoints. These first detailed measurements from cable-breaking flows therefore help to assess and potentially mitigate hazards to submarine cables, such as by identifying a relationship between river floods, tides and cable-breaking turbidity currents, showing that cable-breaking flows may accelerate with distance from shore, and suggesting that cables should be located away from areas of deeper erosion at knickpoints.

## **Acknowledgements**

We are exceptionally grateful to everyone who has assisted with this scientific project, including those who helped to overcome a series of major challenges to recover moorings and data during a global pandemic, after moorings surfaced. They include Jez Evans, Natalie Powney, Guy Dale-Smith, Colin Day, Eleanor Darlington, Paul Provost, Mark Maltby and team at National Marine Facilities, which operates UK scientific research vessels. Michel Senechal (Orange Marine), and Master and crew of the RV Thevenin, who recovered a series of moorings. Alan Ainsworth, Master and crew of the Thor Frigg, who recovered an initial mooring, together with Aymeric Frisch Master and crew of the Maria Francesca, who recovered a final mooring, whilst efforts of Nicholas Ravalac in Point Noire were also very much appreciated. We also thank those who arranged the contract for mooring recovery at short notice, including at the University of Hull, University of Durham (Leila Cole et al.), and NERC. We are also very grateful to Max Boyce (Alacatel Submarine Networks). Takalani Tshivhase (MTN Group), and others for conversations about ongoing cable projects. We are also very grateful Gabriel M. Mokango (Technical Director of Regie des Voies Fluviales in Kinshasa) for access to gauging data for the Congo River, whilst Joao Baptista helped greatly with initial planning. We also thank all those involved in requesting and granting permissions to work in Angolan territorial waters. Finally, we apologise for any omissions, and it has been a real team effort. Research was funded by UK National Environment Research Council (NERC) grants NE/R001952/1 and NE/S010068/1, by a Royal Society Dorothy Hodgkin Fellowship (DHF\R1\180166) to Matthieu Cartigny, and by a Leverhulme Trust Early Career Fellowship (ECF-2018-267) to Ed Pope.

## **References**

1. Carter, L., Gavey, R., Talling, P.J., and Liu, J.T., 2014, Insights into submarine geohazards from breaks in subsea telecommunication cables. *Oceanography*, 27, 58-67.
2. Talling, P.J., Paull, C.K., and Piper D.J.W., 2014. How are subaqueous sediment density flows triggered, what is their internal structure and how does it evolve? Direct observations from monitoring of active flows. *Earth Science Reviews*, 125, 244-287.
3. Talling, P.J., Allin, J., Armitage, D.A., Arnott, R.W.C., Cartigny, M.J.B., Clare, M.A., Felletti, F., Covault, J., Girardclos, S., Hansen, E., Hill, P.R., Hiscott, R.N., Hogg, A.J., Hughes Clarke, J., Jobe, Z.R., Malgesini, G., Mozzato, A., Naruse, H., Parkinson, S., Peel, F.J., Piper, D.W., Pope, E., Postma, G., Rowley, P., Sguazzini, A., Stevenson, C.J., Sumner, E.J., Sylvester, Z., Watts, C., and Xu, J., 2015. Key future directions for research on turbidity currents and their deposits. *Journal of Sedimentary Research*, 85, 153-169.
4. Kuenen, P. H., and Migliorini, C. I., 1950. Turbidity currents as a cause of graded bedding. *The Journal of Geology*, 58(2), 91-127.
5. Heezen, B.C. and Ewing, M., 1952. Turbidity currents and submarine slumps, and the 1929 Grand Banks earthquake. *American Journal of Science*, 250, 849-873.
6. Piper, D. J. W., Cochonat, P. and Morrison, M. L., 1999. The sequence of events around the epicentre of the 1929 Grand Banks earthquake: initiation of debris flows and turbidity current inferred from sidescan sonar. *Sedimentology*, 46, 79-97.
7. Carter, L., Milliman, J.D., Talling, P.J., Gavey, R., and Wynn, R.B., 2012. Near-synchronous and delayed initiation of long run-out submarine sediment flows from a record-breaking river flood, offshore Taiwan. *Geophysical Research Letters* 39, L12603.
8. Gavey, R., Carter, L., Liu, J.T., Talling, P.J., Hsu, R., Pope, E., and Evans, G., 2017. Frequent sediment density flows during 2006 to 2015 triggered by competing seismic and weather cycles: observations from subsea cable breaks off southern Taiwan. *Marine Geology*, 384, 147-158.
9. Clare, M., Lintern, D.G., Rosenberger, K., Hughes Clarke, J.E., Paull, C., Gwiazda, R., Cartigny, M.J.B., Talling, P.J., Perera, D., Xu, J., Parsons, D., Silva Jacinto, R., and Apprioual, R., 2020. Lessons learned from monitoring of turbidity currents and guidance for future platform designs. *Geological Society, London, Special Publications*, 500, <https://doi.org/10.1144/SP500-2019-173>

10. Xu, J.P., Noble, M.A. and Rosenfeld, L.K., 2004. In-situ measurements of velocity structure within turbidity currents. *Geophysical Research Letters*, 31(9).
11. Vangriesheim, A., Khripounoff, A., and Crassous, P., 2009. Turbidity events observed in situ along the Congo submarine channel. *Deep Sea Research Part II*, 56, 2208–2222.
12. Hughes Clarke, J. E., 2016. First wide-angle view of channelized turbidity currents links migrating cyclic steps to flow characteristics. *Nature Communications*, 7, 11896.
13. Azpiroz-Zabala, M., Cartigny, M.J.B., Talling, P.J., Parsons, D.R., Sumner, E.J., Clare, M.A., Simmons, S., Cooper, C., and Pope E.L., 2017. Newly recognised turbidity current structure can explain prolonged flushing of submarine canyons. *Science Advances*, 3, e1700200
14. Paull, C.K., Talling, P.J., Maier, K., Parsons, D., Xu, J., Caress, D., Gwiazda, R., Lundsten, E., Anderson, K., Barry, J., Chaffey, M., O'Reilly, T., Rosenberger, K., Simmons, S., McCann, M., McGann, M., Kieft, B., Gales, J., Sumner, E.J., Clare, M.A., and Cartigny, M.J.B., 2018. Powerful turbidity currents driven by dense basal layers. *Nature Communications*, NCOMMS-18-09895A. doi: 10.1038/s41467-018-06254-6.
15. Heezen, B.C., Menzies, R.J., Schneider, E.D., Ewing, M.W., and Granelip, C.L., 1964. Congo Submarine Canyon. *A.A.P.G. Bulletin*, 48, 1126-1149.
16. Peters, J.J., 1978. Discharge and sand transport in the braided zone of the Zaire Estuary. *Netherlands Journal of Sea Research*, 12, 273-292.
17. Babonneau, N., Savoye, B., Cremer, M., and Klein, B., 2002. Morphology and architecture of the present canyon and channel system of the Zaire deep-sea fan. *Marine and Petroleum Geology*, 19, 445e467.
18. Babonneau, N., Savoye, B., Cremer, M., and Bez, M., 2010. Sedimentary architecture in meanders of a submarine channel: detailed study of the present Congo turbidite channel (Zaiango Project). *Journal of Sedimentary Research*, 80, 852–866.
19. Savoye, B., Babonneau, N., Dennielou, B., and Bez, M., 2009. Geological overview of the Angola-Congo margin, the Congo deep-sea fan and its submarine valleys. *Deep Sea Research Part II: Topical Studies in Oceanography*, 56 (23), 2169e2182.
20. Picot, M., Droz, L., Marsset, T., Dennielou, B., and Bez, M., 2016. Controls on turbidite sedimentation: Insights from a quantitative approach of submarine channel and lobe architecture (Late Quaternary Congo fan). *Marine and Petroleum Geology*, 72, 423e446.
21. Picot, M., Marsset, T., Droz, L., Dennielou, B., Baudin, F., Hermoso, M., de Rafelis, M., Sionneau, T., Cremer, M., Laurent, D., and Bez, M., 2019. Monsoon control on channel avulsions in the Late Quaternary Congo Fan. *Quaternary Science Reviews*, 204, 149e171.
22. Dennielou, B., Droz, L., Babonneau, N., Jacq, C., Bonnel, C., Picot, M., Le Saout, M., Saout, Y., Bez, M., Savoye, B., Olu, K., and Rabouille, C., 2017. Morphology, structure, composition and build-up processes of the active channel-mouth lobe complex of the Congo deep-sea fan with inputs from remotely operated underwater vehicle (ROV) multibeam and video surveys. *Deep Sea Research Part II: Topical Studies in Oceanography*, 142, 25e49.
23. Rabouille, C., Baudin, F., Dennielou, B., and Olu, K., 2017. Organic carbon transfer and ecosystem functioning in the terminal lobes of the Congo deep-sea fan: outcomes of the Congolobe project. *Deep Sea Research Part II: Topical Studies in Oceanography*, 142, 1e6.
24. Rabouille, C., Dennielou, B., Baudin, F., Raimonet, M., Droz, L., Khripounoff, A., Martinez, P., Mejanelle, L., Michalopoulos, P., and Pastor, L., 2019. Carbon and silica megasink in deep-sea sediments of the Congo terminal lobes. *Quaternary Science Reviews*, 222, 105854.
25. Khripounoff, A., Vangriesheim, A., Babonneau, N., Crassous, P., Dennielou, B., and Savoye, B., 2003. Direct observation of intense turbidity current activity in the Zaire submarine valley at 4000 m water depth, *Marine Geology*, 194(3–4), 151-158.
26. Cooper, C., Wood, J., and Andrieux, O., 2013. Turbidity current measurements in the Congo Canyon. *Offshore Technology Conference*, Houston, TX, 6 to 9 May 2013.
27. Cooper, C., Wood J., Imran, J., Islam, A., Wright, P., Faria, R., Tati, A., and Casey, Z., 2016. Designing for turbidity currents in the Congo Canyon. *Offshore Technology Conference*, Houston, TX, 2 to 5 May 2016.
28. Simmons, S. M., Azpiroz-Zabala, M., Cartigny, M. J. B., Clare, M. A., Cooper, C., Parsons, D. R., Pope, E. L., Sumner, E. J., and Talling, P. J., 2020. Novel acoustic method provides first detailed measurements of sediment concentration structure within submarine turbidity currents. *Journal of Geophysical Research*. doi:10.1029/2019JC015904



29. Pope, E.L., Heijnen, M.S., Talling, P.J., Silva Jacinto, R., Baker, M.L., Hage, S., Hasenhündl, M., Heerema, C.J., McGhee, C., Ruffell, S., Simmons, S.M., Cartigny, M.J.B., Clare, M.A., Dennielou, B., Gaillot, A., Parsons, D.R., Peirce, C., and Urlaub, M., 2021. Landslide-dams in submarine canyons can profoundly affect sediment and carbon transfer to the deep-sea. *Nature Geoscience*, in review.
30. [tides.mobilegeographics.com/calendar/year/6162.html?y=2019](https://tides.mobilegeographics.com/calendar/year/6162.html?y=2019)
31. Milliman, J. D., and Farnsworth, K. L., 2011. *River discharge to the coastal ocean: a global synthesis*, Cambridge University Press.
32. Bola, G., Tshimanga, R.M., Trigg, M.A., Neal, J., Hawker, L., Mwamba, L., and Bates P., 2021. Flood frequency analysis in the Congo River Basin, in prep.
33. [www.usgs.gov/natural-hazards/earthquake-hazards/earthquakes](https://www.usgs.gov/natural-hazards/earthquake-hazards/earthquakes)
34. Eisma, D., De Blok, J.W., Dorrestein, R., Postma, H., Nienhuis, P.H., and Weber, R.E., 1978. Geochemical Investigations in the Zaire River, Estuary and Plume. *Netherlands Journal of Sea Research*, 12, 255–420.
35. Clare, M.A., Hughes Clarke, J.E., Talling, P.J., Cartigny, M.J., and Pratomo, D.G., 2016. Preconditioning and triggering of offshore slope failures and turbidity currents revealed by most detailed monitoring yet at a fjord-head delta. *Earth and Planetary Science Letters*, 450, 208-220.
36. Bailey, L.P., Clare, M.A., Rosenberger, K.J., Cartigny, M.J., Talling, P.J., Paull, C.K., Gwiazda, R., Parsons, D.R., Simmons, S.M., Xu, J. and Haigh, I.D., 2021. Preconditioning by sediment accumulation can produce powerful turbidity currents without major external triggers. *Earth and Planetary Science Letters*, 562, 116845.
37. Parker, G., Fukushima, Y., & Pantin, H. M., 1986. Self-accelerating turbidity currents. *Journal of Fluid Mechanics*, 171,145-181.
38. Heerema, C.J., Talling, P.J., Cartigny, M.J., Paull, C.K., Bailey, L., Simmons, S.M., Parsons, D.R., Clare, M.A., Gwiazda, R., Lundsten, E., Anderson, K., Maier, K.L., Xu, J.P., Sumner, E.J., Rosenberger, K., Gales, J., McGann, M., Carter, L., Pope, E., and Monterey Coordinated Canyon Experiment (CCE) Team. 2020. What determines the downstream evolution of turbidity currents? *Earth and Planetary Science Letters*, 532, 116023.
39. Carter, L., 2010. *Submarine cables and the oceans: connecting the world* (No. 31). UNEP/Earthprint.
40. Heijnen, M.S., Clare, M.A., Cartigny, M.J.B., Talling, P.J., Hage, S., Lintern, D.G., Stacey, C., Parsons, D.R., Simmons, S.M., Chen, Y., Sumner, E.J., Dix, J.K., and Hughes Clarke, J.E., 2020. Rapidly-migrating and internally-generated knickpoints can control submarine channel evolution. *Nature Communications*, 11, 3129.

## Figures

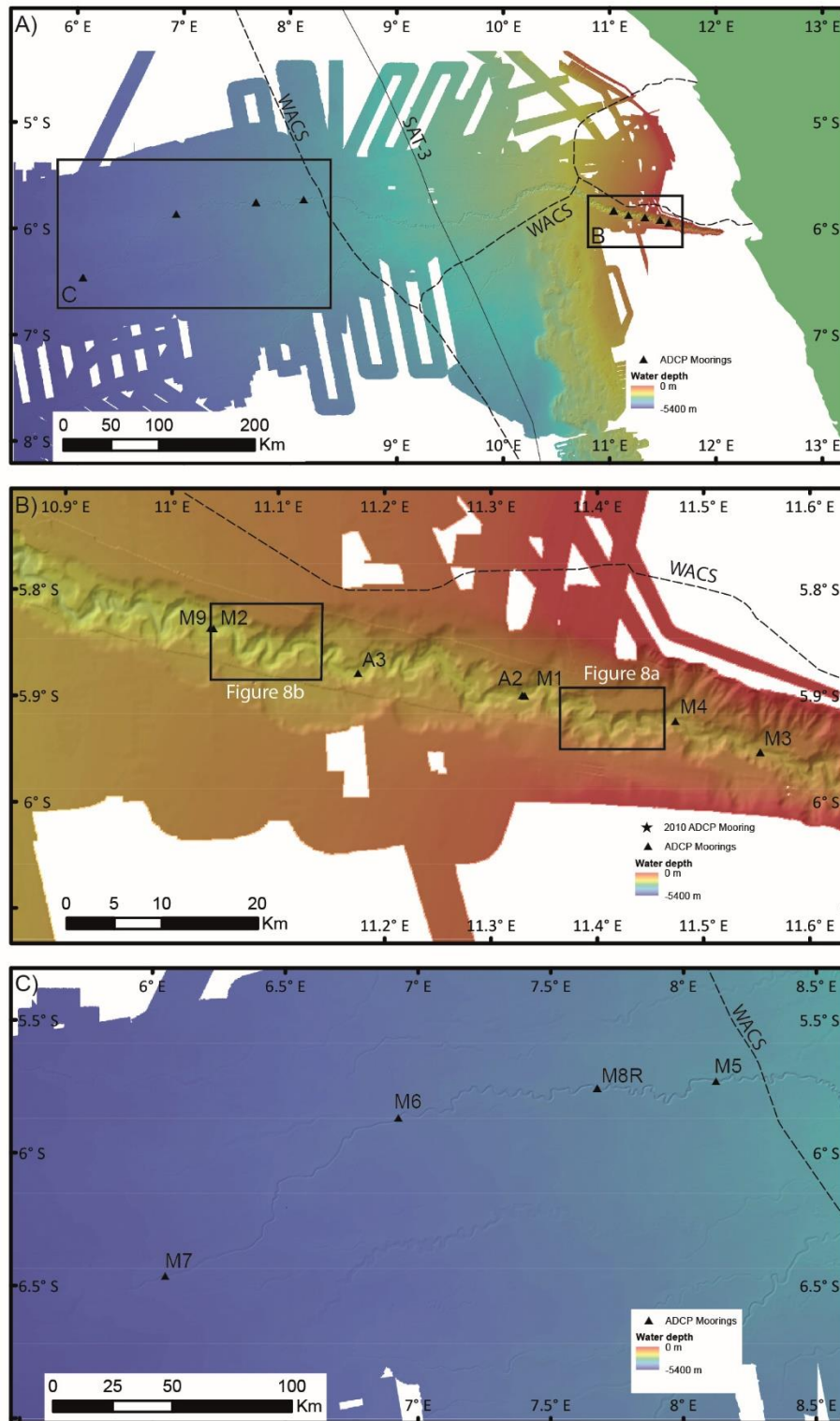


**Figure 1.** Maps of the Congo Submarine Canyon and Channel showing seabed locations of ADCP-moorings (black triangles) deployed in 2019-2020, together with the South Atlantic 3 (SAT-3) and West Africa Cable System (WACS) cables. **(A)** Congo Canyon-Channel offshore West Africa, showing locations of detailed maps. **(B)** Detailed map of upper Congo Canyon, with mooring names (e.g. M3). **(C)** Detailed map of the distal Congo Channel within international waters with mooring names.

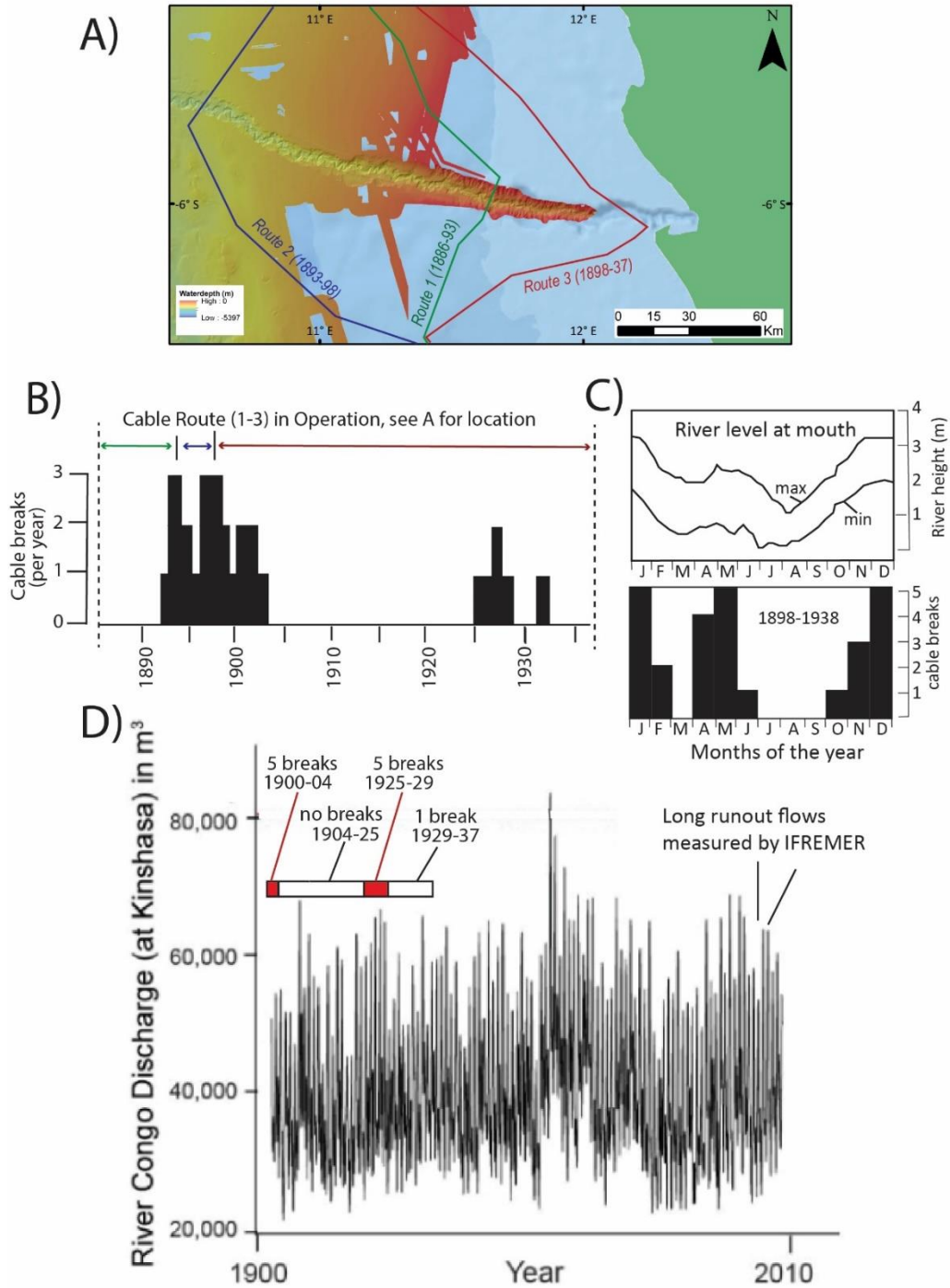


**Figure 2.** Insights into timing, frequency and triggers of turbidity currents in upper Congo Canyon from the location of older (1886 to 1937) seabed cable breaks. These cable routes were located in the upper canyon, closer to shore than the currently active telecommunication cables (Fig. 1). **(A)** Map of upper canyon and river mouth showing three cable routes used from 1886-1893, 1893-1898, and 1898-1937. **(B)** Number of cable breaks each year between 1886 to 1937. **(C)** Monthly changes in Congo River level at a gauging station near its mouth, and total number of cable breaks in each month, from 1898 to 1938. **(D)** Changes in annual maximum discharge of the Congo River at Kinshasa from 1900-2008, compared to periods in which there were five cable breaks red box (1900-1904), no cable breaks (1904-1923), 5 cable breaks (1925-1929), and one cable break (1928-1937). Parts A-C after<sup>15</sup>.

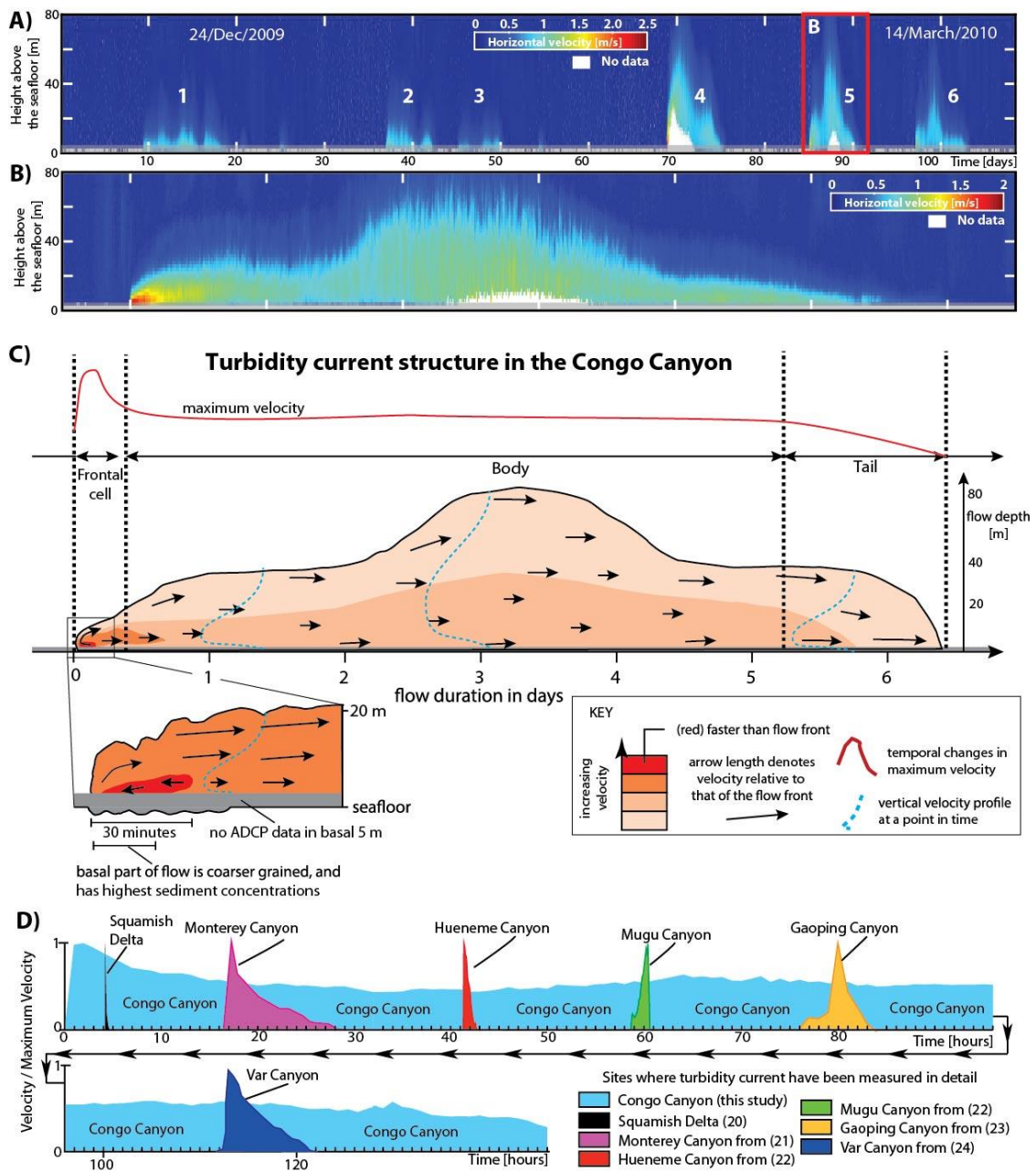


**Figure 3.** Internal structure of a turbidity current in the upper Congo Submarine Canyon, as measured by an ADCP mooring in 2009–2010 (after<sup>13</sup>; location of mooring shown in Figure 1b). This ADCP was located 80m above the seabed, and measured velocity profiles every ~30 secs. **(A)** Full velocity time series for 3-month deployment in 2009–2010, showing turbidity currents were active for ~33% of this period. **(B and C)** Internal structure of an individual turbidity current, labelled flow 5 in (A), with inset showing details of the frontal part. The flow comprises a relatively fast and dense ‘frontal cell’ that runs ahead of a much more prolonged but slower-moving body and tail. Arrows denote relative movement of sediment-laden fluid flow relative to the flow front, showing how the faster frontal cell sheds fluid back into the rest of the trailing flow. The red line shows how maximum flow speed changes over time. **(D)** Turbidity currents that flush the Congo Canyon are far more prolonged than any previously monitored oceanic turbidity current. This panel compares the duration of the upper Congo Canyon flows in 2010 and turbidity currents that have been monitored previously using ADCPs in other shallower water locations. See <sup>13</sup> and <sup>28</sup> for further details.



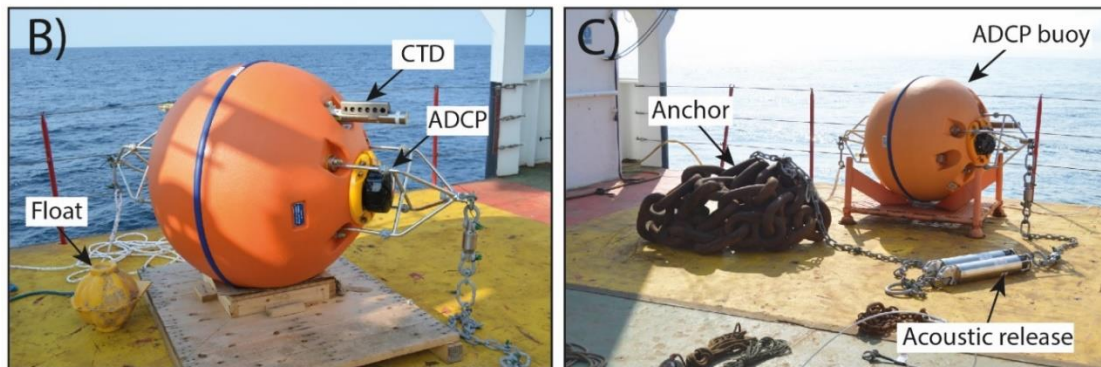
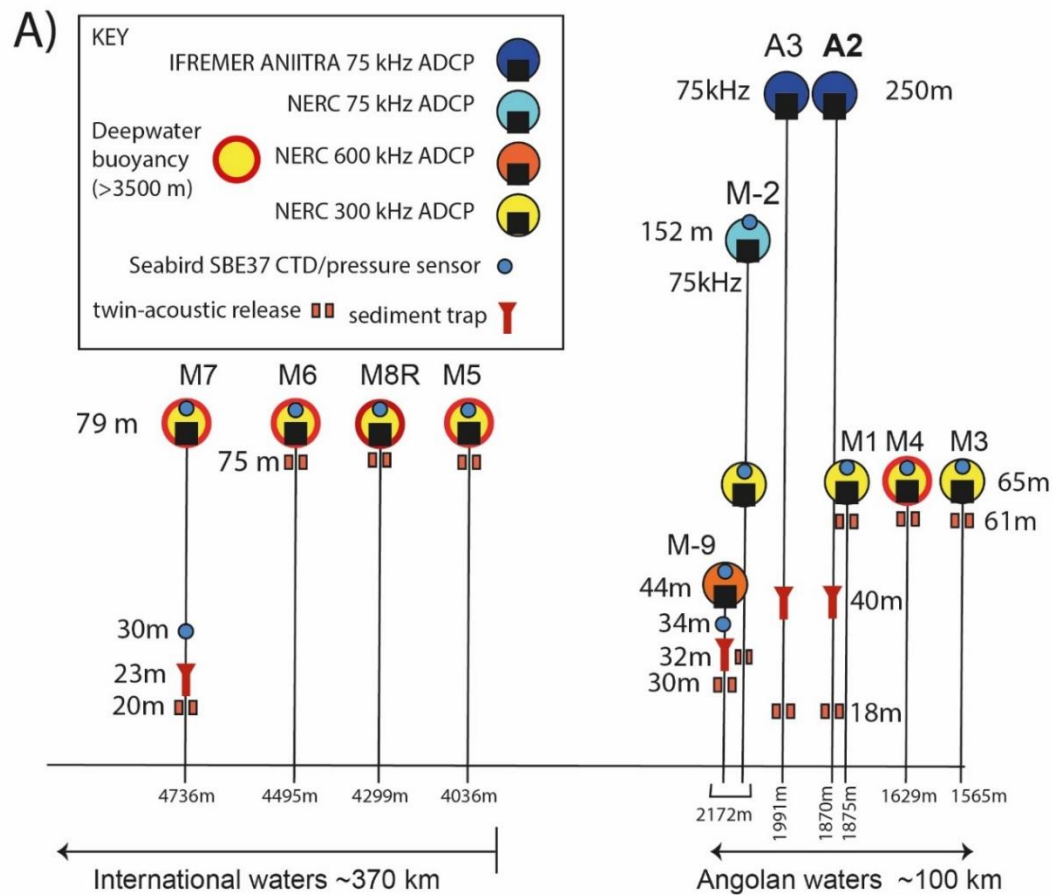


**Figure 4. (A)** Summary diagram of the array of 11 moorings deployed along the Congo Canyon-Channel in 2019-2020. Seven moorings were deployed in shallow, Angolan waters in the upper canyon (right side), and four moorings were deployed in deeper, international waters (left side). The diagram shows the type of ADCP and other sensors included in each mooring, and their heights above the seabed. Water depths of mooring anchors are shown, together with positions of sediment traps, and acoustic releases for recovery. However, all moorings surfaced after their wire was broken by turbidity currents, on the various dates shown in Figure 5. **(B and C)** Photographs of moorings on deck before deployments in 2019, showing the anchor, buoyant float that houses the ADCP and CTD sensors, and the two acoustic releases, which are all linked via chain or wire.

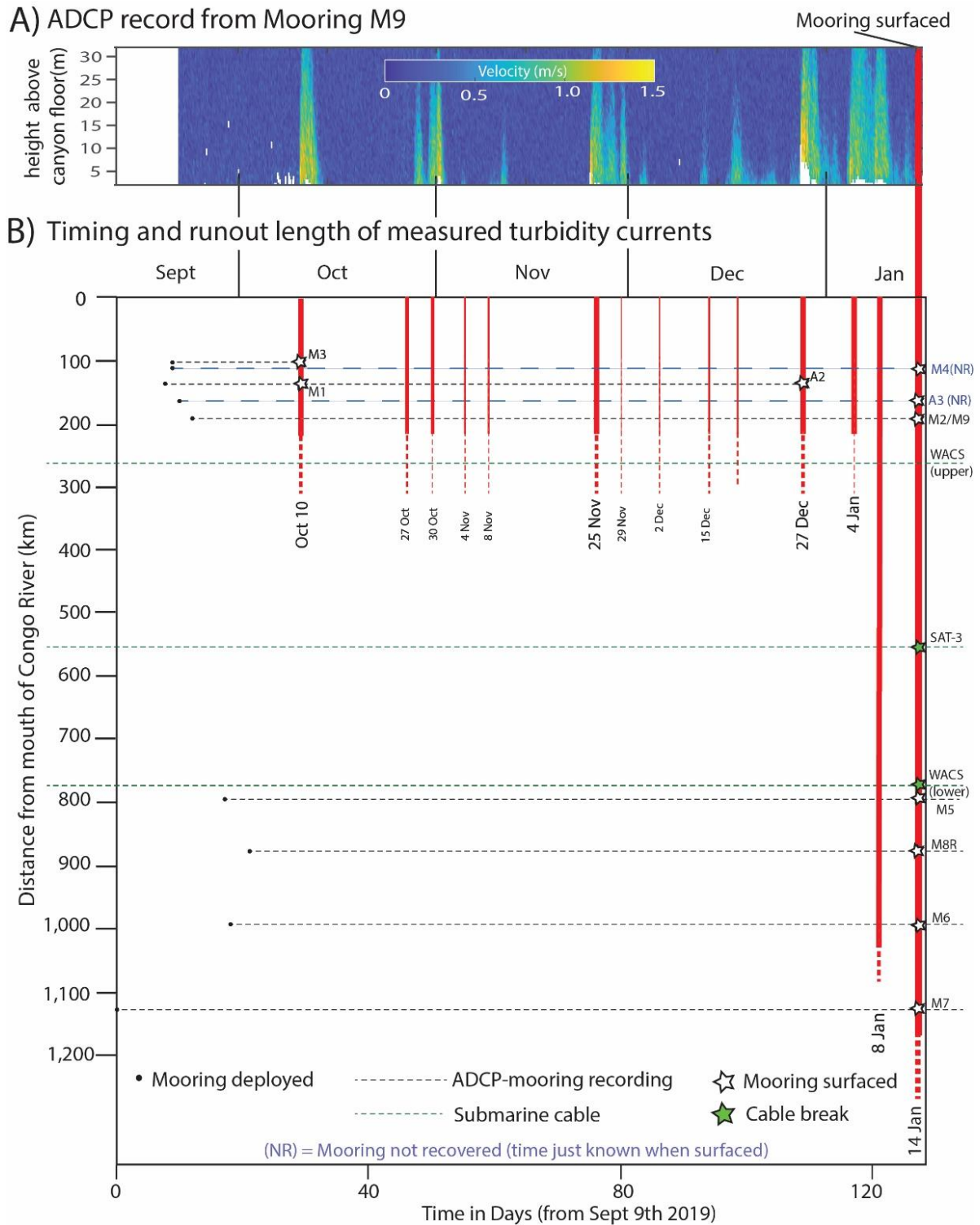


**Figure 5.** Timing, character and runout distance of turbidity currents measured from September 2019 to January 2020 along the full Congo Canyon-Channel system (see Figure 1). **(A)** ADCP time series of velocities measured at mooring M9. **(B)** Plot of event times against distance from Congo River mouth, as measured along the sinuous canyon-channel axis. Red vertical lines denote flow events, and indicate their runout distances, with the most powerful 14-16<sup>th</sup> January event in bold. Dotted horizontal lines (at a specific distance) denote a mooring site or submarine cable. Times of mooring deployment are shown, together with when moorings broke and surfaced due to flows. Two moorings (M4 and A3) were not recovered ('NR'); flow timings at these sites are derived from when mooring reached the ocean surface, and reported locations.

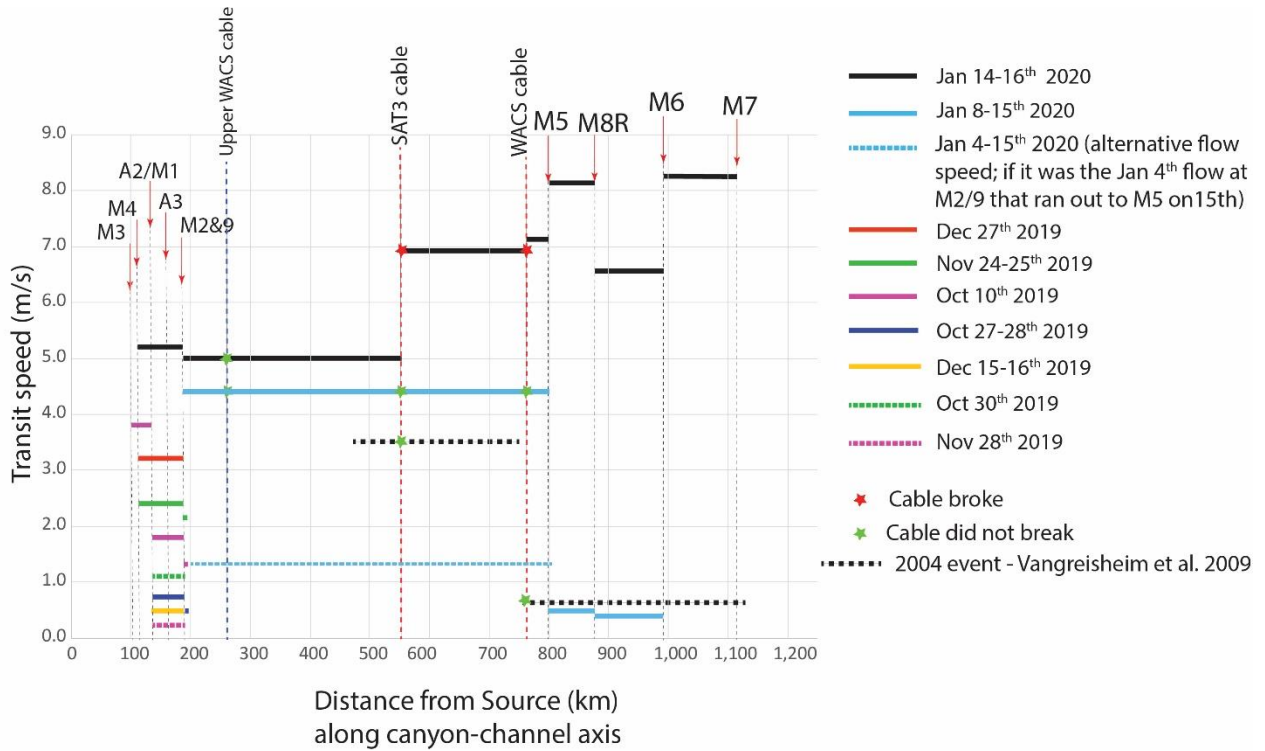


**Figure 6.** Changes in transit (flow front) speeds of turbidity current events with distance from the Congo River mouth. Flow speeds are derived from the timing of submarine cable breaks, and flow arrival times at moored ADCPs. Two moorings (M4 and A3) were not recovered; flow timings at these sites are derived from when mooring reached the ocean surface, and assume a rise rate of 150 m/min (as seen in other mooring recoveries). Distances are measured along the sinuous course of the Congo Canyon-Channel. Seabed telecommunication cable are shown by vertical dashed lines, and ADCP-mooring (e.g. M7) sites are shown by red arrows and vertical dashed lines. Turbidity currents in 2019-2020 are shown by coloured solid lines, and information from a study of a turbidity current in 2004 (by Vangreishem et al., 2009) is shown by a dashed black line. Two potential speeds are shown for the 4/8<sup>th</sup> to 15<sup>th</sup> January turbidity current between moorings M2&9 to M5. This is because it is unclear whether it was the flow recorded at mooring M2&9 on 4<sup>th</sup> January, or on 8<sup>th</sup> January, which was the turbidity current that reached mooring M5 on 15<sup>th</sup> January.

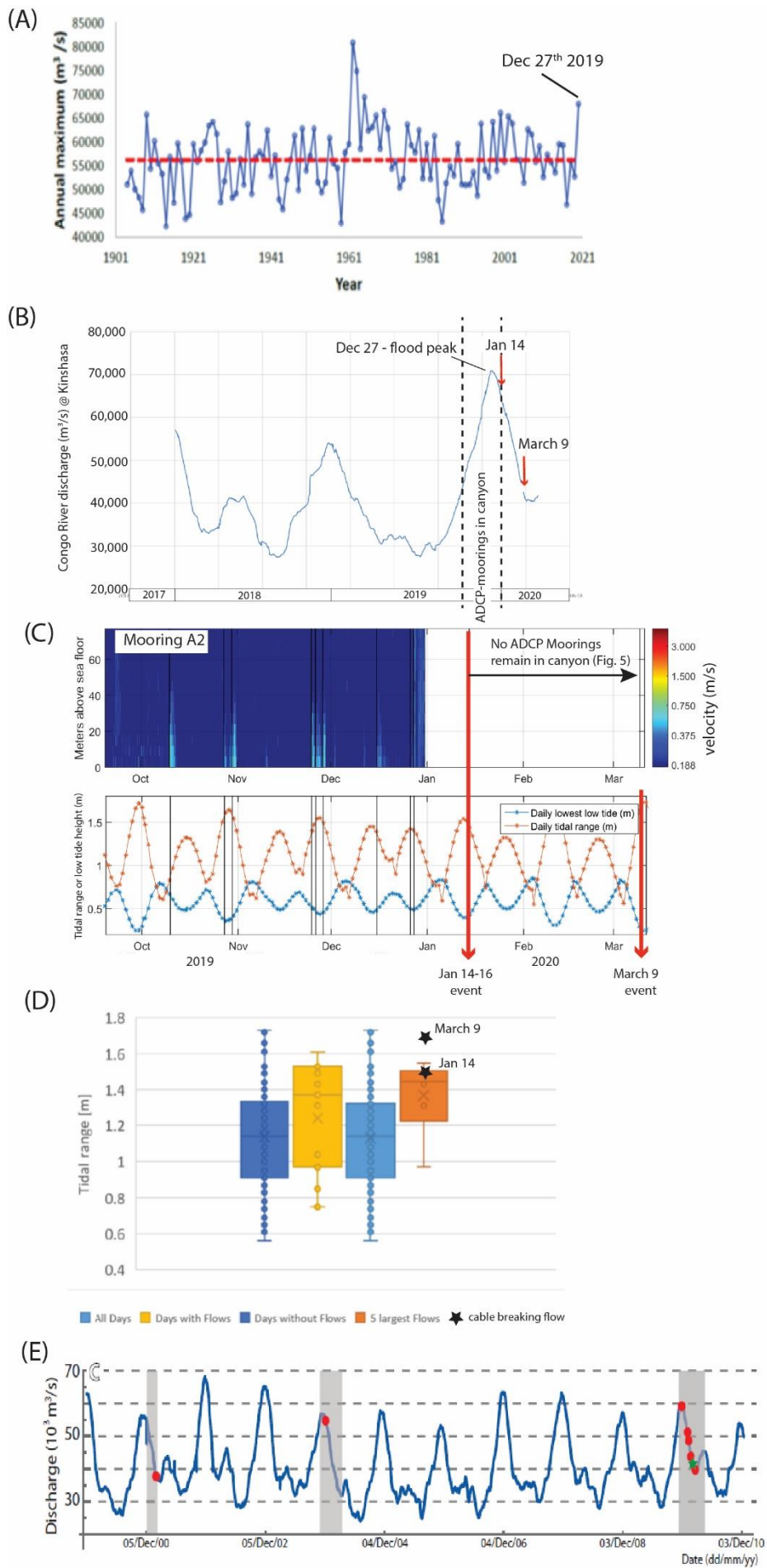




**Figure 7.** Triggering of turbidity currents by river flood and spring tides. **(A)** Maximum annual discharge of the Congo River measured at Kinshasa from 1900-2021, with the average value shown by red dotted line. **(B)** Fluctuations of Congo River discharge at Kinshasa from January 2018 to April 2020, showing a major flood peak in late December 2019. This flood peak probably took another 2-3 days to reach the river mouth. **(C)** Turbidity current events recorded between 19<sup>th</sup> September 2019 and 14-16<sup>th</sup> January 2020, based on ADCP-mooring data and cable breaks. The upper panel is an ADCP time series of velocity profiles (faster speeds in warmer colours), measured through time at mooring A2. The ADCP mooring floated to the sea surface due to the 27<sup>th</sup> December flow, hence data stops. Lower panel shows spring-neap tidal cycles, with changes in the elevation of minimum low tides (blue line), and the total tidal range (orange line), each day at Santo Antonio (Soyo) in Angola ([tides.mobilegeographics.com/calendar/year/6162.html?y=2019](https://tides.mobilegeographics.com/calendar/year/6162.html?y=2019)). **(D)** Daily tidal range at Santo Antonio (Soyo) in the estuary as box and whisker plots for: all days in which ADCP-moorings were in the Congo Canyon in 2019-2020, days on which turbidity currents were likely triggered at the river mouth (see text for uncertainties), days with no triggering of turbidity currents at the river mouth, and days on which the four longest and fastest flows were triggered. Each (standard box and whisker plot) shows the median tidal range (x), tidal ranges on given days (o), and the 95% percentile of the distribution of tidal ranges for specified days (-). Stars indicate two cable breaking flows in January and March 2020. **(E)** Timing of turbidity currents (red dots) measured either at 1850 m water depth in upper canyon (after<sup>13</sup>), or by earlier IFREMER projects in deeper water (after<sup>11,25</sup>). Periods in which moorings were present and recording are shown by grey bars, and green star is the flow shown in Figure 3B-C.

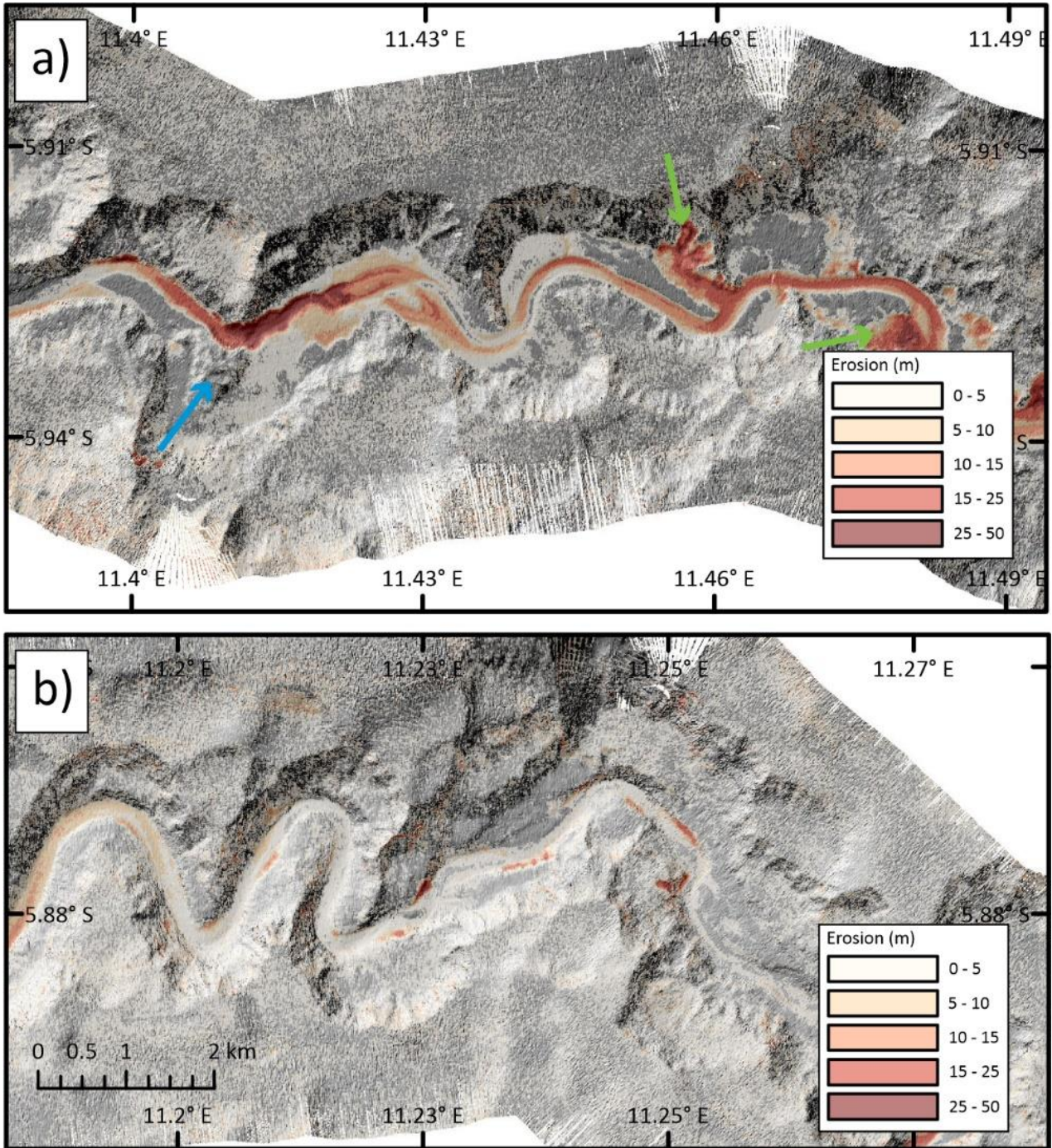


**Figure 8.** Maps of changes in seabed elevation, and patterns of localised seabed erosion, for two sections of the upper Congo Canyon between September 2019 and October 2020. Depth of erosion is shown in red, with (hillshaded) bathymetry from 2019 shown underneath in grey-scale. **(A)** Location where deep erosion in 2019-2020 is associated with knickpoints (steeper zones in canyon long-profile), between moorings M4 and A2/M1 (Fig. 1b). Note also the prominent canyon side-wall failures in 2019-2020 (green arrows), and an older (pre-2019) landslide-dam (blue arrow) that created a major knickpoint<sup>29</sup>. **(B)** Location between moorings A3 and M2/9 (Fig. 1b) where turbidity currents in 2019-2020 caused much less erosion of the canyon floor. It may be advantageous to locate cable crossing away from areas of deep erosion associated with knickpoints.



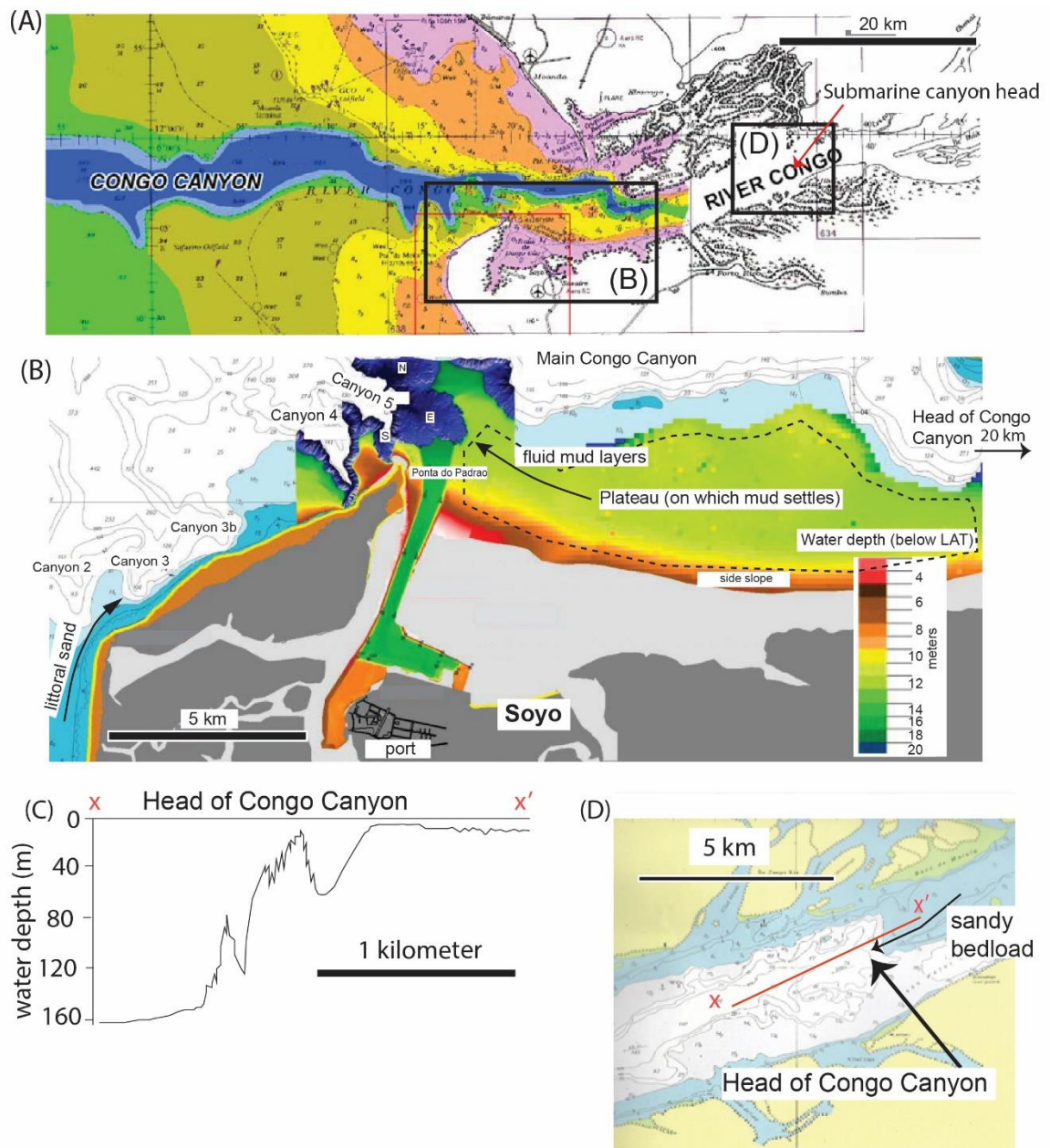


**Figure 9.** (A) Map of the Congo River Estuary and Submarine Canyon showing the locations of parts B and D. (B) Detailed map of the estuary mouth area offshore from Soyo, showing water depth below lowest astronomical tide (LAT), including the submerged plateau (dotted line) on which mud settles from the Congo River plume. This mud can form fluid-mud layers that enter Canyons 4 and 5. Smaller volumes of sand are carried by littoral currents along the coast into Canyons 2 and 3. (C and D) Map and bathymetric cross section across the head of the Congo Canyon, where water depths abruptly increase from ~20 to ~160 m. Large amounts of sand are carried as bedload from the river and into the canyon head.